Ozone isotopic composition: an angular effect in scattering processes?

C. Camy-Peyret, F. Robert

Annales Geophysicae (2001) 19: 229–244 © European Geophysical Society 2001

Annales Geophysicae

Ozone isotopic composition: an angular effect in scattering processes?

F. Robert[1] **and C. Camy-Peyret**[2]

[1]CNRS-Muséum, Laboratoire de Minéralogie, 61 rue Buffon, 75005 Paris, France
[2]CNRS-Laboratoire de Physique moléculaire et applications, Université Pierre et Marie Curie, Tour 13, Bte 76 - 4 place Jussieu, 75252 Paris Cedex 05, France

Received: 19 June 2000 – Revised: 5 December 2000 – Accepted: 11 December 2000

Abstract. The ratio of the differential scattering cross sections involving distinguishable and indistinguishable isotopes may exhibit non-mass dependent angular variations. A numerical application of this hypotheses to the ozone reaction rates reproduces some of the results observed in laboratory experiments. This theory could be tested through a cross beam experiment where the isotopic composition of the scattered products is recorded as a function of their scattering angles.

Key words. Atmospheric composition and structure (middle atmosphere – composition and chemistry)

Glossary

General formalism

– A and B: two isotopes of the same chemical element
– XA and XB: two isotopically substituted molecules
– [A] and [XA]: the number densities of A and XA, respectively
– *R* as subscript: stands for reactive. Used for reactions yielding an exchange of isotopes such as A + XB → XA+ B
– *NR* as subscript: stands for non-reactive. Used for reactions which do not yield an isotope exchange such as A+ XB → A + XB
– *T* as subscript: stands for total
– $k_{\mathrm{A-XB},R}$: isotopic exchange rate constant
– α: isotopic fractionation factor
– θ and $\pi - \theta$: the scattering angle expressed in coordinates of the center of mass frame (see Figs. 1 and 3)
– θ_{XA}: the scattering angle of XA
– $F(\theta)$: the differential cross section describing the particle scattering at a collisional angle θ and at relative velocity v. Usually reported in the literature as $F(\theta) = |f(\theta)|^2$
– Φ_i: in the cross beam experiments, the flux of species i
– x_i: the relative isotopic abundance of isotope i $\left(\sum x_i = 1\right)$
– $\beta(\theta) = 1/2\{F_T(\theta) + F_T(\pi - \theta)\}/F_T(\theta)$
– Θ: the range of scattering angles, $\Theta = [\theta_1, \theta_2]$
– $k(\Theta)$: the rate constant for reactions between distinguishable isotopes for a given distribution of speeds and angles; noted $\langle F(\theta, v)\rangle$ in the text

$$k(\Theta) = \int_0^\infty v f(v) dv \int_{\theta_1}^{\theta_2} [F_{NR}(\theta, v) + F_R(\theta, v)] \sin\theta d\theta$$

– $k_i(\Theta)$: the rate constant for reactions between indistinguishable isotopes for a given distribution of speeds and angles: $1/2\{F_T(\theta) + F_T(\pi - \theta)\}$ in place of $F_{NR}(\theta) + F_R(\theta)$ in $k(\Theta)$
– $\beta(\Theta) = k_i(\Theta)/k(\Theta)$

General relations

– $F_{NR}(\theta) + F_R(\theta) = F_T(\theta)$
– $F_{NR}(\pi - \theta) + F_R(\pi - \theta) = F_T(\pi - \theta)$
– $G(\theta) = 1/2\{F_T(\theta) + F_T(\pi - \theta)\}$
– If $\Theta = [0, \pi]$, $\quad k(\Theta) = k_i(\Theta)$, $\quad \beta(\Theta) = 1$

Ozone formalism

– ^{16}O, ^{17}O and ^{18}O: the three isotopes of oxygen
– [O_2], [O], [M], [O_3^*]: the number densities of molecular O_2, atomic O, the third body M and of activated complex, respectively
– k^*: the rate constant for the formation of the activated complex O_3^*
– $k_D(\Theta)$: the rate constant for the spontaneous dissociation of the activated complex, in a scattering domain of angles Θ, resulting from interactions involving distinguishable isotopes
– $k_{i,D}(\Theta)$: the rate constant for the spontaneous dissociation of the activated complex, in a scattering domain of angles Θ, resulting from interactions involving indistinguishable isotopes
– k_{M}: the rate constant for the reaction of O_3^* with the third body M, leading to the stabilization of ozone.

Correspondence to: F. Robert (robert@mnhn.fr)

1 Introduction

The first measurement of mass independent oxygen isotopic fractionation was reported by Clayton et al (1973) in the high temperature minerals of carbonaceous meteorites. In 1980 Cicerone and McCrumb (1980) reported an ^{18}O enrichment in atmospheric ozone. Mauersberger (1981, 1987) measured enrichments in the $^{18}O/^{16}O$ ratio of stratospheric ozone relative to that of atmospheric oxygen, and came to the decisive conclusion according to which such an enrichment cannot be explained by the standard theory of isotope fractionation. Krankowsky et al. (2000) have shown that stratospheric ozone exhibits an isotopic fractionation in perfect agreement with laboratory determinations but somewhat lower than those measured in 1981. A crucial step in understanding this effect was made by Thiemens and Heidenreich (1983) and Heidenreich and Thiemens (1986) who demonstrated that the isotope distribution in ozone was non-mass dependent, i.e. that the relative isotopic fractionation for $^{17}O/^{16}O$ was equal to that for $^{18}O/^{16}O$. Such a relation between the two oxygen isotopic ratios was in disagreement with all known isotope fractionation mechanisms. Indeed, all these mechanisms yield a mass dependent isotope fractionation, i.e. a relative variation in the $^{17}O/^{16}O$ ratio of 1% should be accompanied by a 2% variation in the $^{18}O/^{16}O$ ratio. Clearly the theory developed by Urey (1947) and Bigeleisen (1947) for isotope fractionation in thermodynamical equilibrium and in kinetic processes, respectively, does not predict these isotope effects (see also Kaye and Strobel, 1983; Kaye, 1986).

Additional measurements in natural ozone by Mauersberger (1987), Abbas et al. (1987), Goldman et al. (1989), Goldman et al. (1998), Schueler et al. (1990) have confirmed the mass independent isotopic fractionation in ozone, although these analyses showed large differences in the isotopic fractionation factor. Numerous laboratory studies using mass spectrometry (Morton et al., 1989; Morton et al., 1990; Thiemens and Jackson, 1987; Thiemens and Jackson, 1990; Yang and Epstein, 1987), diode laser technique (Anderson et al., 1985) and infrared absorption (Bahou et al., 1997) have shown enrichment in the heavy isotopomers of ozone.

Several attempts to reconcile the isotope fractionation theory with these observations have been made. For example, a proposal of Valentini (1987) involved nonadiabatic transitions from Π or Δ molecular electronic states to Σ electronic states. This explanation was rejected by Morton et al. (1989) based on detailed laboratory studies where the excited electronic states did not contribute to the synthesis of ozone. Bates (1988) argued against these explanations and suggests that the lifetime of symmetrical and unsymmetrical activated complexes are different because of the lack of randomization of their internal energies. Recently, Gellene (1996) proposed a model of symmetry-induced kinetic isotope effects. According to this model, when a homonuclear diatomic molecule is involved in the $O + O_2$ reaction, only a fraction of the rotational states correlate with those in the ozone molecule, yielding a depression of the rate constant of this reaction relative to those involving heteronuclear molecules. But this explanation is in conflict with recent experimental results (Mauersberger et al., 1999). Although the physical reason for these anomalies remains unknown, it has been suggested that a mechanism involving a modification of the classical recombinaison theory (Anderson et al., 1985; Bates, 1988; Heidenrich and Thiemens, 1986; Gellene, 1996) or the formation of electronically excited ozone (Anderson et al., 1992; Anderson and Mauersberger, 1995) during the $O + O_2$ collisions was necessary (see also the recent reviews by Thiemens (1999) and Mauersberger et al. (1999), in the introduction of their 1999 article).

In the present paper we will follow another approach proposed by Robert et al. (1988) and Robert and Baudon (1990) in which there is no need for consideration of symmetry of the O_2 or O_3 molecules. Contrary to the previous approaches, we will show that a specific aspect of isotopic reactions has been omitted in the theoretical treatment of isotopic fractionation. In the usual theory it is assumed that no difference (beside the usual mass difference between isotopes) can exist between the scattering cross sections of the different isotopes of the same element, because the interaction potential of isotopic species is essentially the same. In fact, a marked difference does exist between the collision cross sections involving distinguishable and indistinguishable isotopes. This effect remains a "classical" effect. We will show that several laboratory data can be reproduced numerically if one assume that this difference is at the origin of the isotope effects observed during the synthesis of ozone. To emphasize this point, we have purposely ignored other isotope effects (Sehested et al., 1995; Anderson et al., 1997; Bahou et al., 1997) which have been shown to contribute to the overall ozone isotopic fractionation.

Therefore, throughout the paper we will consider that the three isotopes of oxygen have the same mass, i.e. can be distinguished essentially by their "names": 16, 17 and 18. By neglecting the mass difference, we will put into focus the marked differences in the behavior of isotopes considered now as individual particles (distinguishable or not), with no reference to the type of chemical bound they are involved into. Using this unique assumption we will show that some of the experimentally observed isotopic fractionation can be numerically reproduced within the framework of the classical model for ozone reaction rates. The validity of the present approach remains to be tested by a more rigorous quantum mechanical calculation (which is not the purpose of this paper).

2 General formulation for atom-diatom isotopic exchange

2.1 Preliminary remarks

All formula and letters are defined in the glossary and may not be repeated in the text. For the sake of clarity, we will initially neglect the mass difference between different iso-

topes of the same element. This approximation permits several simplifications in the formalism developed in the following, but will not be repeated when it applies. It should be kept in mind that no isotopic fractionation is expected within this assumption because all known isotope effects depends ultimately upon this mass difference which determines the internal energy differences between the isotopically substituted molecules. It is also important to understand that within this assumption all the isotopic cross sections for isotopically substituted molecules are strictly equal.

2.2 Mass dependent isotopic fractionation in equilibrium and in kinetic processes

2.2.1 Thermodynamic equilibrium

The rate of a bimolecular isotope exchange reaction

$$\mathrm{A} + \mathrm{XB} \xrightarrow{k_{\mathrm{A-XB},R}} \mathrm{B} + \mathrm{XA} \tag{1}$$

is generally considered as a weighted mean contribution of rates of individual process for all the internal states (reactants and products). In Eq. (1) k stands for the rate constant and the subscript R (R stands for reactive) indicates that an isotopic exchange takes place in the course of the reaction A + XB. For simplicity, the dependence with temperature (usually noted $k(T)$ in the literature) is omitted in our notation. A reaction rate similar to (1) can be written for B involved in the reverse reaction

$$\mathrm{B} + \mathrm{XA} \xrightarrow{k_{\mathrm{B-XA},R}} \mathrm{A} + \mathrm{XB}\,. \tag{2}$$

By definition the isotopic fractionation factor is

$$\alpha = k_{\mathrm{A-XB},R}/k_{\mathrm{B-XA},R}\,. \tag{3}$$

Since the differences in the isotopic masses are neglected, $\alpha = 1$ in (3) indicates that no isotope fractionation is expected under thermodynamic equilibrium. At equilibrium for an isolated system involving only reactions (1) and (2), the isotopic abundances are related by the relation

$$\alpha = ([\mathrm{B}]/[\mathrm{A}])\,/\,([\mathrm{XB}]/[\mathrm{XA}])\ . \tag{4}$$

Introducing the masses of the reactants in Eq. (3), yields the common isotope fractionation effect for which α is slightly different from unity because of small differences in the internal states of the different isotopic molecules.

2.2.2 Kinetic processes

In kinetic processes the isotopic fractionation is supposed to take place between the activated complex (noted *) and the reactants. Such a process is illustrated by the following reactions:

$$\mathrm{A} + \mathrm{XB} \xrightarrow{k^*_{\mathrm{A-XB},R}} \mathrm{AX}\ldots\mathrm{B}^*\,, \tag{5}$$

$$\mathrm{A} + \mathrm{XB} \xrightarrow{k^*_{\mathrm{A-XB},NR}} \mathrm{A}\ldots\mathrm{XB}^*\,, \tag{6}$$

$$\mathrm{A} + \mathrm{XA} \xrightarrow{k^*_{\mathrm{A-XA},T}} \mathrm{A}\ldots\mathrm{X}\ldots\mathrm{A}^*\,. \tag{7}$$

An exchange of isotopes may (reaction 5) or may not (reaction 6) take place during the reaction between A and XB (subscript NR for the non-reactive reaction). The total rate constant (subscript T) is used to describe reaction (7) involving identical isotopes (A + XA) because it is impossible to decide if an isotopic exchange took place or not during the reaction. This total rate constant is always supposed to be the sum of the reactive and the non-reactive processes

$$k^*_{\mathrm{A-XA},T} = k^*_{\mathrm{A-XA},R} + k^*_{\mathrm{A-XA},NR}\,. \tag{8}$$

In a mixture of A, B, XA and XB, the rate of disappearance of A occurring via the formation of the activated complex can be written

$$-d[\mathrm{A}]/dt = k^*_{\mathrm{A-XB},R}[\mathrm{A}][\mathrm{XB}] + k^*_{\mathrm{A-XB},NR}[\mathrm{A}][\mathrm{XB}] + k^*_{\mathrm{A-XA},T}[\mathrm{A}][\mathrm{XA}]\,. \tag{9}$$

A similar equation can be written for $-d[\mathrm{B}]/dt$. The ratio of the disappearance rates is then

$$(-d[\mathrm{A}]/-d[\mathrm{B}])/([\mathrm{A}]/[\mathrm{B}]) = \{k^*_{\mathrm{A-XB},T}[\mathrm{XB}] + k^*_{\mathrm{A-XA},T}[\mathrm{XA}]\}/\{k^*_{\mathrm{B-XA},T}[\mathrm{XA}] + k^*_{\mathrm{B-XB},T}[\mathrm{XB}]\}\,. \tag{10}$$

Since in our idealized system, the isotopic masses are neglected

$$k^*_{\mathrm{B-XA},T} = k^*_{\mathrm{B-XB},T} = k^*_{\mathrm{A-XB},T} = k^*_{\mathrm{A-XA},T} \tag{11}$$

and Eq. (10) becomes

$$\{(-d[\mathrm{A}]/-d[\mathrm{B}])/([\mathrm{A}]/[\mathrm{B}])\} = 1\,. \tag{12}$$

Equation (12) indicates that no isotopic fractionation takes place during the formation of the activated complex. Introducing the isotopic masses in (10) yields the usual isotopic fractionation effect for which

$$\{(-d[\mathrm{A}]/-d[\mathrm{B}])/([\mathrm{A}]/[\mathrm{B}])\} \neq 1\,. \tag{13}$$

Therefore, mass effects yield, both in equilibrium and in kinetic processes, the so called "mass dependent fractionation effect" (see "introduction" for this definition). Such an effect is not considered in the present paper.

2.3 Possible origin of the mass independent isotope effect

The isotopic effect we wish to describe here is entirely caused by reactions involving indistinguishable isotopes (such A+ XA). More specifically, it is linked to a difference in the distribution in space of the products of reactions involving distinguishable and indistinguishable isotopic species.

Consider the distribution in space of the products when the reactants are isotopically distinguishable. Such a situation can be illustrated by the encounter of a beam of XA molecules with a beam of B atoms:

$$\xrightarrow{\mathrm{XA}}\ \xleftarrow{\mathrm{B}}$$

In Fig. 1 we use this idealized experiment to define the parameters of the collision:

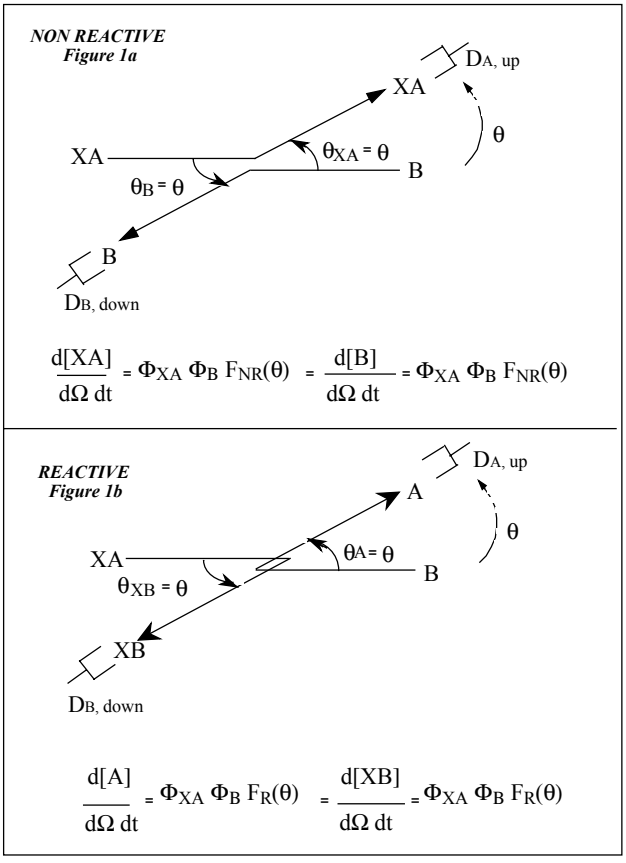

Fig. 1. Schematic diagram of the trajectory of different isotopic species as a function of their scattering angles in a cross beam experiment between XA and B. A and B are two isotopes of the same element. "Reactive" indicates that isotopes are exchanged in the course of the collision. A and XA are detected by D_{A} and B and XB by D_{B}. The differential scattering cross section measured by D_{A} and D_{B} are strictly equal at $\theta_{\mathrm{XA}} = \theta_{\mathrm{B}} = \theta$.

(1) The angles of the collision θ_{XA} and θ_{B} (see Fig. 1a), defined in the co-ordinates of the center of mass of the atom molecule system, are expressed relative to the directions of the isotopes A or B in the beams *before* the collision. For simplicity, scattering is described only for the two spatial dimensions; azimutal angles are not introduced in the formalism. Since we are only interested in reactions between isotopes, the spectator atom X plays no role and its possible collision with B is not considered.

(2) Two detectors noted D_{A} and D_{B} in Fig. 1 (in opposite direction in the center of mass reference), measure the flux of the scattered species; D_{A} records A and XA while D_{B} records B and XB. In principle, the atom A and the molecule XA can be distinguished by the detector D_{A} and similarly for D_{B}. This classical experiment allows the determination of the differential scattering cross sections, i.e. the variations of the fluxes of A or XA as a function of θ_{A} or θ_{XA}, and the variations of the fluxes of B or XB as a function of θ_{B} or θ_{XB}. We note $F(\theta)$ the differential cross section as a function of the scattering angle θ (see glossary for definition).

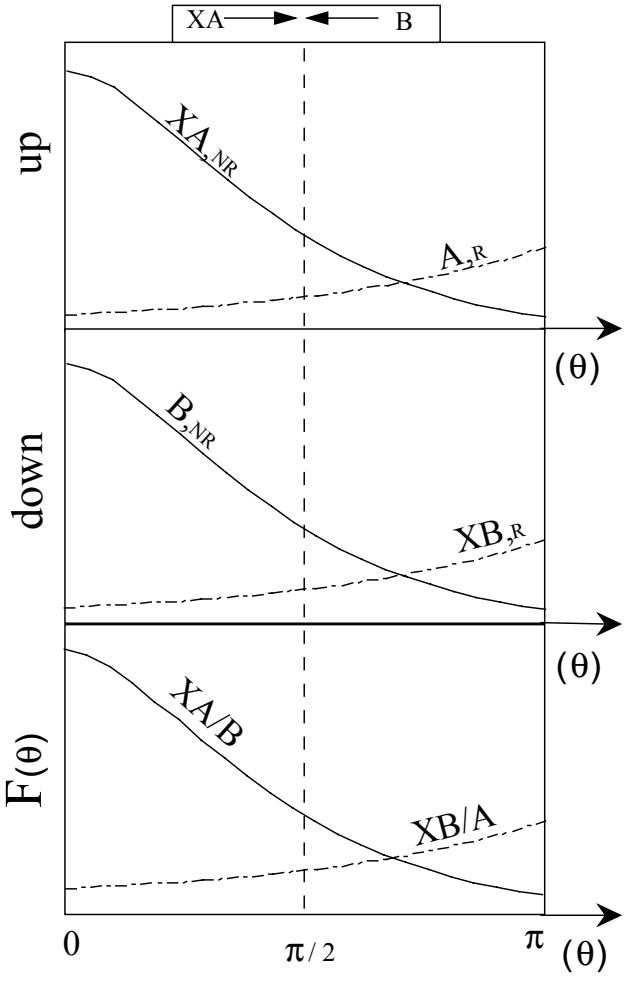

Fig. 2. Schematic diagram of the isotopic distributions of XA, XB, A and B, as a function of their scattering angles in the cross beam experiment shown in Fig. 1. The probability for detecting XA and B at $\theta_{\mathrm{XA}} = \theta_{\mathrm{B}} = \theta$ are strictly equal (and similarly for XB and A). The reactive and non-reactive overall differential cross sections are reported in the lower part of the figure.

(3) As shown in Fig. 1, two reactions can occur and the products of these reactions detected by D_{A} and D_{B} are

$$\mathrm{XA} + \mathrm{B} \rightarrow \mathrm{XA}\ (\text{at } \theta_{\mathrm{XA}} \text{ in } D_{\mathrm{A},NR}) + \mathrm{B}\ (\text{at } \theta_{\mathrm{B}} \text{ in } D_{\mathrm{B},NR}) \quad \text{Fig. 1a} \quad (14)$$

$$\mathrm{XA} + \mathrm{B} \rightarrow \mathrm{XB}\ (\text{at } \theta_{\mathrm{XB}} \text{ in } D_{\mathrm{B},R}) + \mathrm{A}\ (\text{at } \theta_{\mathrm{A}} \text{ in } D_{\mathrm{A},R}) \quad \text{Fig. 1b} \quad (15)$$

As for cross sections, *NR* and *R* stand for non-reactive and reactive reactions, respectively. In such an experiment the two products of the same encounter are detected "simultaneously", since if we are to get a molecule in the position θ there must be an atom in the opposite side at the angle $\pi - \theta$. Therefore, the distributions as a function of θ for atoms and molecules resulting from the same reaction are strictly equal.

(4) We note Φ_i the flux of species i.

Using these definitions, the differential number of molecules or atoms (per solid angle Ω and unit time t) scattered by

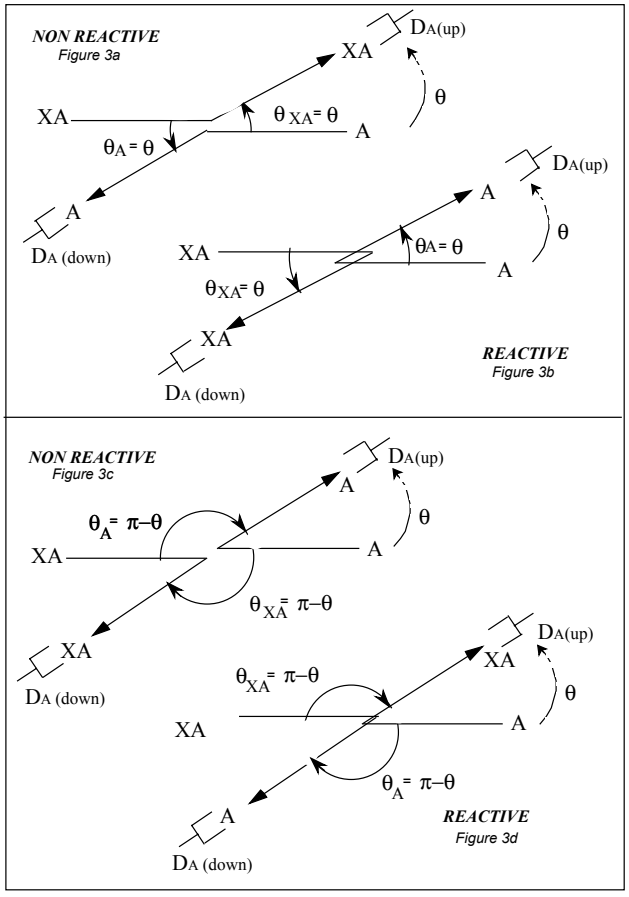

Fig. 3. Schematic diagram of the trajectory of different isotopic species as a function of their scattering angles in a cross beam experiment between XA and A. A and XA are detected by the upper and lower detectors D_{A}. As for the reactions between XA and B, the differential scattering cross sections measured by the upper and lower detectors D_{A} are strictly equal.

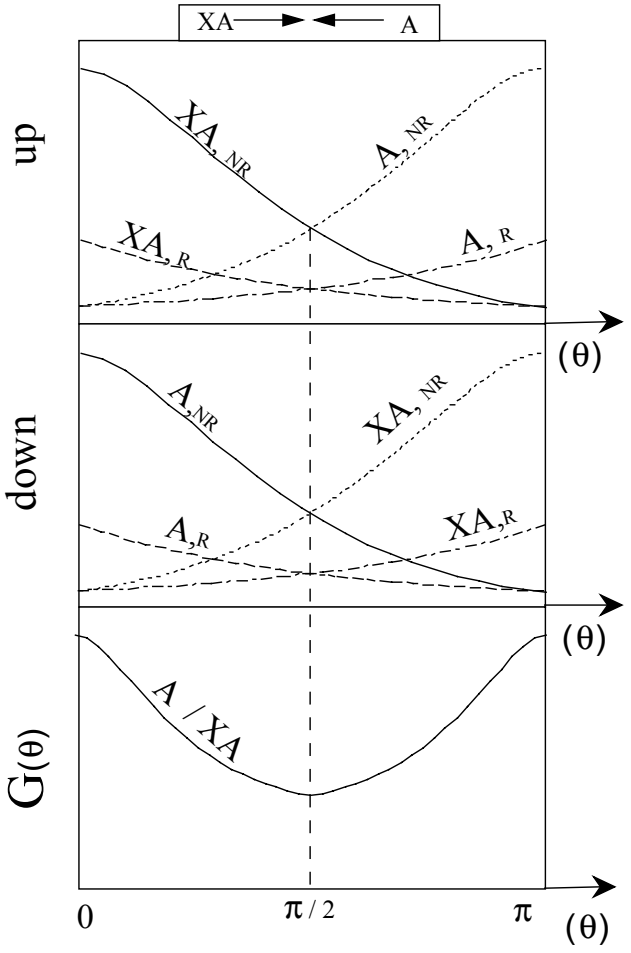

Fig. 4. Schematic diagram of the isotopic distributions of XA and A as a function of their scattering angles in the cross beam experiment shown in Fig. 3. Although drawn for heuristic purposes, XA and A resulting from reactive and non-reactive reactions cannot be experimentally distinguished. "Reactive" indicates that isotopes are exchanged in the course of the collision. The resulting overall differential cross section $G(\theta) = 1/2\{F_T(\theta) + F_T(\pi - \theta)\}$ describing the reactions between A and XA is drawn in the lower part of the figure. $G(\theta)$ exhibits a marked enhancement around $\theta = \pi$ as compared to $F(\theta)$ (see Fig. 2).

these two reactions, for a given initial relative velocity, are

$$d[\mathrm{XA}]/d\Omega dt = d[\mathrm{B}]/d\Omega dt = \Phi_{\mathrm{XA}}\Phi_{\mathrm{B}}F_{NR}(\theta)\,, \qquad (16)$$

$$d[\mathrm{XB}]/d\Omega dt = d[\mathrm{A}]/d\Omega dt = \Phi_{\mathrm{XA}}\Phi_{\mathrm{B}}F_{R}(\theta)\,. \qquad (17)$$

In such a situation $F_{NR}(\theta)$ and $F_R(\theta)$ are clearly different since they correspond to different pairs of molecule/atom products, i.e. XA/B and XB/A, scattered in opposite directions. Schematic diagrams of $F(\theta)$ for atoms and molecules scattered in space by the two reactions (14) and (15) are reported in Fig. 2.

One could also introduce in the theory the "impact parameter" to describe the distribution in space of the products of the collisions. This impact parameter is omitted here because it is entirely dictated by the relative velocity v and the scattering angle, which are the explicit parameters of the cross sections we will use hereafter.

Consider now the same experiment with A in place of B:

$$\xrightarrow{\mathrm{XA}}\ \xleftarrow{\mathrm{A}}$$

In such a case, two reactions which were not detectable in the previous experiment, can now be detected by the two detectors D_{A}. These reactions are shown in Fig. 3. These two reactions are the reactive and non-reactive reactions at the scattering angle $\pi - \theta$. To ease the discussion, let us designate arbitrarily D_{A}(up) and D_{A}(down) the upper and lower detectors in Fig. 3, since these two detectors can always be experimentally distinguished. The following reactions will be detected:

$$\mathrm{XA} + \mathrm{A} \rightarrow \mathrm{XA}\ (\theta_{\mathrm{XA}}\ \text{in}\ D_{\mathrm{A},NR}(\mathrm{up})) + \mathrm{A}\ (\theta_{\mathrm{A}}\ \text{in}\ D_{\mathrm{A},NR}(\mathrm{down}))\quad \text{Fig. 3a} \qquad (18)$$

$$\mathrm{XA} + \mathrm{A} \rightarrow \mathrm{XA}\ (\theta_{\mathrm{XA}}\ \text{in}\ D_{\mathrm{A},R}(\mathrm{down})) + \mathrm{A}\ (\theta_{\mathrm{A}}\ \text{in}\ D_{\mathrm{A},R}(\mathrm{up}))\quad \text{Fig. 3b} \qquad (19)$$

$$XA + A \rightarrow XA\ (\theta_{XA} \text{ in } D_{A,NR}(\text{down})) + A\ (\theta_A \text{ in } D_{A,NR}(\text{up}))\quad \text{Fig. 3c} \quad (20)$$

$$XA + A \rightarrow XA\ (\theta_{XA} \text{ in } D_{A,R}(\text{up})) + A\ (\theta_A \text{ in } D_{A,R}(\text{down}))\quad \text{Fig. 3d} \quad (21)$$

When a species A (and similarly for XA) is detected at any angle it is impossible to tell if the individual scattering process was reactive or non-reactive (see Figs. 3b, c). This is different from the same individual process for distinguishable isotopes for which there is no ambiguity to asses that a reactive collision occurred if A is detected. Schematic diagrams of the functions $F(\theta)$ for atoms and molecules scattered in space by these four reactions are reported in Fig. 4. At this stage, we have therefore reached the central (and unique) assumption of the paper: the total cross section must be used to describe the reaction A + XA. This assumption is illustrated in the lower part of the Fig. 4 where the cross sections for the reactions A − XA are constructed using exactly the same rules defined for the reactions between A and XB.

The differential number of molecules or atoms scattered by these four reactions are

$$d[XA]/d\Omega dt = d[A]/d\Omega dt = \Phi_{XA}\Phi_A 1/2\{F_{NR}(\theta) + F_{NR}(\pi-\theta) + F_R(\theta) + F_R(\pi-\theta)\}. \quad (22)$$

Since $F_{NR}(\theta) + F_R(\theta) = F_T(\theta)$

$$d[XA]/d\Omega dt = d[A]/d\Omega dt = \Phi_{XA}\Phi_A 1/2\{F_T(\theta) + F_T(\pi-\theta)\} = \Phi_{XA}\Phi_A G(\theta). \quad (23)$$

The factor 1/2 is introduced in (22) since we have to consider four possible reactions between XA and A and only two between XA and B. This factor 1/2 is also introduced in classical mechanics to prevent a double counting when the particles are identical.

Using these results, it is possible to predict the isotopic composition of atoms and molecules as a function of their scattering angle in the following idealized experiment:

$$\xrightarrow{\text{XA, XB}} \quad \xleftarrow{\text{A, B}}$$

The following reactions should take place:

$$A + XA \rightarrow A + XA \qquad 1/2\{F_T(\theta) + F_T(\pi-\theta)\} = G(\theta) \quad (24)$$

$$B + XB \rightarrow B + XB \qquad 1/2\{F_T(\theta) + F_T(\pi-\theta)\} = G(\theta) \quad (25)$$

$$A + XB \rightarrow A + XB \qquad F_{NR}(\theta) \quad (26)$$

$$A + XB \rightarrow B + XA \qquad F_R(\theta) \quad (27)$$

$$B + XA \rightarrow B + XA \qquad F_{NR}(\theta) \quad (28)$$

$$B + XA \rightarrow A + XB \qquad F_R(\theta) \quad (29)$$

The corresponding cross sections are indicated for each reactions. According to our formalism the molecular products of these reactions *at the same angle* $\theta = \theta_{XA} = \theta_{XB}$ are

$$d[XA]/d\Omega dt = \Phi_{XA}\Phi_B F_{NR}(\theta) + \Phi_{XB}\Phi_A F_R(\theta) + \Phi_{XA}\Phi_A 1/2\{F_T(\theta) + F_T(\pi-\theta)\}, \quad (30)$$

$$d[XB]/d\Omega dt = \Phi_{XB}\Phi_A F_{NR}(\theta) + \Phi_{XA}\Phi_B F_R(\theta) + \Phi_{XB}\Phi_B 1/2\{F_T(\theta) + F_T(\pi-\theta)\}. \quad (31)$$

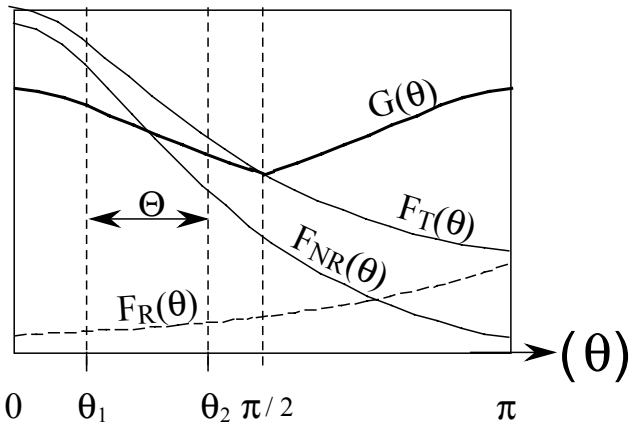

Fig. 5. Schematic differential cross sections for $F_{NR}(\theta)$, $F_R(\theta)$, $F_T(\theta) = F_{NR}(\theta) + F_R(\theta)$ and $G(\theta) = 1/2\{F_T(\theta) + F_T(\pi-\theta)\}$. F functions stand for distinguishable isotopic reactions and G for undistinguishable. The domain $\Theta = [\theta_1, \theta_2]$ marks the domain of angle where the activated complex cannot possibly stabilize. Since $G(\theta) \neq F_T(\theta)$, an isotopic fractionation as a function of the scattering angle is expected.

Let us assume for simplicity that there is no isotopic fractionation between the beams

$$\Phi_{XA}\Phi_B = \Phi_{XB}\Phi_A. \quad (32)$$

Then, the production rate ratio $d[XA]/d[XB]$ is

$$(d[XA]/d[XB])/(\Phi_{XA}/\Phi_{XB}) = \{x_B + x_A\beta(\theta)\}/\{x_A + x_B\beta(\theta)\} \quad (33)$$

with

$$\beta(\theta) = 1/2\{F_T(\theta) + F_T(\pi-\theta)\}/F_T(\theta) = G(\theta)/F_T(\theta) \quad (34)$$

and with x_A and x_B the relative abundance of the isotopes A and B

$$x_A + x_B = 1 \quad (35)$$

for a chemical element having two isotopes.

In quantum mechanics, $\beta(\theta)$ can be $\neq 1$ because $F_T(\theta)$ is not symmetrical around $\pi/2$ (as shown from the individual $F_R(\theta)$ and $F_{NR}(\theta)$ in Fig. 2). Therefore, $G(\theta)$ is markedly different from $F_T(\theta)$ and an isotopic fractionation is expected as a function of the scattering angle, i.e.

$$(d[XA]/d[XB])/(\Phi_{XA}/\Phi_{XB}) \neq 1. \quad (36)$$

$G(\theta)$ and $F_T(\theta)$ are compared in Fig. 5. Note that in classical mechanics, as for example in the case of the scattering of rigid spheres, $F_T(\theta)$ does not vary with θ and Eq. (34) is equal to unity, i.e. no isotopic fractionation is expected as a function of the scattering angle θ.

The theoretical result of Eq. (33) can be tested in a cross beam experiment where the isotopic compositions of the scattered species are measured as a function of their scattering angles.

Suppose that these isotopic reactions take place in a real mixture and are followed by a chemical reaction whose products are selected according to the scattering angles of the isotopic species (i.e. according to their internal energy after the reaction). In such an angular selection, the fraction of the reactants which return to the initial mixture can be described by the following reaction

$$\mathrm{A} + \mathrm{XB} \xrightarrow{k(\Theta)} \mathrm{A} + \mathrm{XB} \ \ (\text{or } \mathrm{B} + \mathrm{XA})\,. \tag{37}$$

Θ designates the domain of scattering angles lying between θ_1 and θ_2 (see Fig. 5) where A and XB are not stabilized in the form of a new chemical species ($\Theta = [\theta_1, \theta_2]$). An isotope exchange may or may not occur during the reaction; hence the notation "or B + XA".

In Fig. 5, it can be observed that in the forward scattering interval $\Theta = [0, \theta_1]$, $G(\theta) < F_T(\theta)$ whereas in most of the backward scattering interval $\Theta = [\theta_2, \pi]$, one has $G(\theta) > F_T(\theta)$. This illustrates the fact that, depending on the considered system, i.e. depending on the width and position of Θ, isotopic enhancement is scattering angle dependent.

The corresponding rate constant $k(\Theta)$ describing the isotopic composition of atoms and molecules that return to the mixture is the result of averaging $F_T(\theta, v)$ over the appropriate distribution of speeds and angles

$$k(\Theta) = \langle F_T(\theta, v)\rangle \quad \text{(see glossary for definitions)}. \tag{38}$$

In such conditions $\beta(\Theta)$ can be defined as

$$\beta(\Theta) = k_i(\Theta)/k(\Theta) \tag{39}$$

with

$$k_i(\Theta) = \langle G(\theta, v)\rangle\,. \tag{40}$$

$k(\Theta)$ and $k_i(\Theta)$ stand for the rate constants involving distinguishable and indistinguishable isotopes, respectively. We will show in the next section that, if $\beta(\Theta)$ is known, the isotopic composition of these atoms and molecules can be calculated. Note also that, if the integration is performed over all the scattering angles ($\Theta = [0, \pi]$), no isotopic fractionation is expected and, as in classical mechanics

$$\beta(\Theta) = 1. \tag{41}$$

From (33) it can be seen that this type of isotopic fractionation will rely entirely on the relative isotopic abundance of a chemical element and thus, can be defined as an "abundance dependent" isotopic fractionation. It should be noted that the isotope effect resulting from (34) is in accordance with the Pauli exclusion principle according to which it is not "permitted" to separate in the calculation, the cross section describing the incident from the recoil particle, if the two particles are indistinguishable.

3 Theoretical application to ozone formation

3.1 Reaction rate model

In order to simplify the formalism, the classical model for the formation rate of ozone will be used. The mass independent isotopic fractionation expected from the theory developed in the preceding section will be used within the framework of this model.

This model is derived from the three following reactions:

$$\mathrm{O} + \mathrm{O_2} \rightarrow \mathrm{O_3^*} \qquad k^* \tag{42}$$

$$\mathrm{O_3^*} \rightarrow \mathrm{O} + \mathrm{O_2} \qquad k_D(\Theta) \tag{43}$$

$$\mathrm{O_3^*} + \mathrm{M} \rightarrow \mathrm{O_3} + \mathrm{M} \qquad k_\mathrm{M} \tag{44}$$

Equation (42) describes the formation of the activated complex $\mathrm{O_3^*}$ with the rate constant k^*. Equation (43) represents the spontaneous dissociation of the complex with the rate constant $k_D(\Theta)$ (D for dissociation); its inverse $1/k_D(\Theta)$ characterizes the lifetime of the complex. In the present treatment we assume that the dissociation of the complex is possible only in a scattering angle domain Θ (see the definition of Θ in the glossary); hence the notation $k_D(\Theta)$. Equation (44) corresponds to the possible stabilization of $\mathrm{O_3^*}$ by a third body M bringing out the proper amount of internal energy. The overall formation rate of ozone is derived assuming that the concentration of the activated complex $\mathrm{O_3^*}$ is constant (steady state), that is

$$d[\mathrm{O_3^*}]/dt = 0\,. \tag{45}$$

Under this condition we have

$$k^*[\mathrm{O}][\mathrm{O_2}] - k_D(\Theta)[\mathrm{O_3^*}] - k_\mathrm{M}[\mathrm{O_3^*}][\mathrm{M}] = 0 \tag{46}$$

and the production rate of $\mathrm{O_3}$ is

$$d[\mathrm{O_3}]/dt = [\mathrm{O_3^*}][\mathrm{M}]\,k_\mathrm{M}\,. \tag{47}$$

From Eqs. (46) and (47), the rate of the overall reaction

$$\mathrm{O} + \mathrm{O_2} + \mathrm{M} \rightarrow \mathrm{O_3^*} + \mathrm{M} \tag{48}$$

can be derived

$$d[\mathrm{O_3}]/dt = [\mathrm{O_2}][\mathrm{O}]\{k^* k_\mathrm{M}[\mathrm{M}]/(k_D(\Theta) + k_\mathrm{M}[\mathrm{M}])\}\,. \tag{49}$$

In the case of the "low pressure approximation" $k_\mathrm{M}[\mathrm{M}] \ll k_D(\Theta)$

$$d[\mathrm{O_3}]/dt = [\mathrm{O_2}][\mathrm{O}]\{k^* k_\mathrm{M}[\mathrm{M}]/k_D(\Theta)\}\,. \tag{50}$$

The usual three body recombinaison rate is recovered in this case as

$$k^{\mathrm{M}}_{\mathrm{O+O_2}} = k^* k_{\mathrm{M}} / k_D(\Theta) \tag{51}$$

and the value recommended by DeMore et al. (1997) will be used for the numerical applications

$$k^{\mathrm{M}}_{\mathrm{O+O_2}}(300\ \mathrm{K}) = (6.0 \pm 0.5) \cdot 10^{-34}\ \mathrm{cm^6 molecule^{-2} s^{-1}} \tag{52}$$

with the following temperature dependence

$$k^{\mathrm{M}}_{\mathrm{O+O_2}}(T) = k^{\mathrm{M}}_{\mathrm{O+O_2}}(300\ \mathrm{K}) \cdot \left(\frac{300\ \mathrm{K}}{T}\right)^{2.3\pm0.5} \mathrm{cm^6 molecule^{-2} s^{-1}}\,. \tag{53}$$

In the case of the "high pressure approximation" $k_{\mathrm{M}}[\mathrm{M}] \gg k_D(\Theta)$ and

$$d[\mathrm{O_3}]/dt = [\mathrm{O_2}][\mathrm{O}]\,k^*\,. \tag{54}$$

3.2 Formalism for isotopic reactions

In this section we write the general rules for the reactions involving all the possible isotopic substitutions in $\mathrm{O_3}$. In order to reduce the number of possible reactions, the three isotopes of oxygen (^{16}O, ^{17}O, ^{18}O) are designated by A, B and C. With this notation, the entire system can be described by four types of reactions: A + AA, A + AB, A + BC and A + BB. As compared to the previous discussion on isotopic exchanges involving A + XB or A + XA, we now consider that X can be A, B or C. For simplicity in the forthcoming reactions, the third body M will be omitted in the reactions of complex stabilization; hence the use of the notation $k_{\mathrm{M}}[\mathrm{M}]$.

The goal of the following paragraphs is to provide a basis for calculating the appropriate formation rate $d[\mathrm{ABC}]/dt$ of the various isotopomers of $\mathrm{O_3}$ using equations similar to (49).

3.2.1 Reaction between indistinguishable isotopes

(1) A + AA:

$$\mathrm{A} + \boldsymbol{A}\boldsymbol{A} \xrightarrow{k^*} \mathrm{AAA}^* \tag{55}$$

$$\mathrm{AAA}^* \xrightarrow{k_{i,D}(\Theta)} \mathrm{A} + \mathrm{AA} \tag{56}$$

$$\mathrm{AAA}^* \xrightarrow{k_{\mathrm{M}}[\mathrm{M}]} \mathrm{AAA} \tag{57}$$

This reaction involves only indistinguishable isotopes. In this case we designate the decomposition rate by $k_{i,D}(\Theta)$.

(2) A + AB:

$$\mathrm{A} + \boldsymbol{A}\mathrm{B} \xrightarrow{1/2yk^*} \mathrm{A}\boldsymbol{A}\mathrm{B}^* \tag{58}$$

$$\mathrm{A}\boldsymbol{A}\mathrm{B}^* \xrightarrow{k_{i,D}(\Theta)} \mathrm{A} + \mathrm{AB} \tag{59}$$

$$\mathrm{A}\boldsymbol{A}\mathrm{B}^* \xrightarrow{k_{\mathrm{M}}[\mathrm{M}]} \mathrm{A}\boldsymbol{A}\mathrm{B} \tag{60}$$

The factor 1/2 in (58) indicates that the probability of having a collision with A is exactly equal to the probability of having the same collision with B in the heteronuclear molecule AB. Each reaction of A with one of the two atoms of AB is thus counted separately and bold italic is used in this discussion to designate the knock-on atom. In our notations we designate the middle atom as the apex of the isosceles triangle which is the normal equilibrium configuration of ozone in its ground electronic state.

The factor y is introduced here because it is assumed that the activated complex has only two channels to be rearranged into its stable form

$$\mathrm{A}\boldsymbol{A}\mathrm{B}^* \rightarrow \mathrm{A}\boldsymbol{A}\mathrm{B}\,, \tag{61}$$

$$\mathrm{A}\boldsymbol{A}\mathrm{B}^* \rightarrow \boldsymbol{A}\mathrm{BA}\,. \tag{62}$$

The incident atom can be (1) either attached to the knock-on atom of the molecule (with a branching ratio y) (2) either attached to the spectator atom of the molecule (with a branching ratio $1 - y$) or (3) inserted between the knock-on and the spectator atom. We neglect this third possibility (see Bahou et al., 1997, for the experimental determination of this contribution). Thus, the other stabilizing channel is

$$\mathrm{A} + \boldsymbol{A}\mathrm{B} \xrightarrow{1/2(1-y)k^*} \boldsymbol{A}\mathrm{BA}^*\,, \tag{63}$$

$$\boldsymbol{A}\mathrm{BA}^* \xrightarrow{k_{i,D}(\Theta)} \mathrm{A} + \mathrm{AB}\,, \tag{64}$$

$$\boldsymbol{A}\mathrm{BA}^* \xrightarrow{k_{\mathrm{M}}[\mathrm{M}]} \boldsymbol{A}\mathrm{BA}\,. \tag{65}$$

There are only two possible rearrangements of the complex and thus

$$yk^* + (1-y)k^* = k^*\,. \tag{66}$$

3.2.2 Reaction between distinguishable isotopes

(1) A + BA:

$$\mathrm{A} + \boldsymbol{B}\mathrm{A} \xrightarrow{1/2yk^*} \mathrm{A}\boldsymbol{B}\mathrm{A}^* \tag{67}$$

$$\mathrm{A}\boldsymbol{B}\mathrm{A}^* \xrightarrow{k_D(\Theta)} \mathrm{A} + \mathrm{BA}\ (\text{or } \mathrm{B} + \mathrm{AA}) \tag{68}$$

$$\mathrm{A}\boldsymbol{B}\mathrm{A}^* \xrightarrow{k_{\mathrm{M}}[\mathrm{M}]} \mathrm{A}\boldsymbol{B}\mathrm{A}\ (\text{or } \boldsymbol{B}\mathrm{AA} \text{ via } (1-y)k^*) \tag{69}$$

Exchange and non-exchange processes are not counted separately in (68) since they do not cause any isotopic fractionation between the activated complex and the reactants beside usual mass dependent effects; hence, the notation "or B + AA".

(2) A + BC:

$$\mathrm{A} + \boldsymbol{B}\mathrm{C} \xrightarrow{1/2yk^*} \mathrm{A}\boldsymbol{B}\mathrm{C}^* \tag{70}$$

$$\mathrm{A}\boldsymbol{B}\mathrm{C}^* \xrightarrow{k_D(\Theta)} \mathrm{A} + \mathrm{BC}\ (\text{or } \mathrm{B} + \mathrm{CA} \text{ or } \mathrm{C} + \mathrm{AB}) \tag{71}$$

$$\mathrm{A}\boldsymbol{B}\mathrm{C}^* \xrightarrow{k_{\mathrm{M}}[\mathrm{M}]} \mathrm{A}\boldsymbol{B}\mathrm{C}\ (\text{or } \boldsymbol{B}\mathrm{CA} \text{ via } (1-y)k^*) \tag{72}$$

Similarly, the reaction with the second atom C can be written using the same rules.

(3) A + BB:

$$\mathrm{A} + \boldsymbol{B}\mathrm{B} \xrightarrow{1/2k^*} \mathrm{A}\boldsymbol{B}\mathrm{B}^* \tag{73}$$

$$\mathrm{A}\boldsymbol{B}\mathrm{B}^* \xrightarrow{k_D(\Theta)} \mathrm{A} + \mathrm{BB}\ (\text{or B} + \mathrm{AB}) \tag{74}$$

$$\mathrm{A}\boldsymbol{B}\mathrm{B}^* \xrightarrow{k_\mathrm{M}[\mathrm{M}]} \mathrm{A}\boldsymbol{B}\mathrm{B}\ (\text{or } \boldsymbol{B}\mathrm{BA}) \tag{75}$$

In this case the two isotopomers are the same (A$\boldsymbol{B}$B and $\boldsymbol{B}$BA); hence, the branching ratio y is not appearing.

3.3 Interpretation of the formalism for isotopic reactions

All the rules defined by Eqs. (55) to (75) are based on a single idea: the ozone isotopic composition is entirely governed by a statistical distribution of isotopes between the reactants. We simply assume that the decomposition of the activated complex is not possible at all angles and therefore, that its decomposition rate cannot be counted similarly if its formation involves distinguishable or indistinguishable isotopes. In the following we discuss the physical significance of the four constants k^*, $k_{i,D}(\Theta)$, $k_D(\Theta)$ and $k_\mathrm{M}[\mathrm{M}]$.

3.3.1 The constant k^*

For all the reactions, we consider that the activated molecules are formed by all the possible collisions between atoms and molecules, occurring at all angles. There is no need to discriminate the rate constants for the formation of the activated complex by reactions involving distinguishable and indistinguishable isotopes; hence, the use of the same constant k^*, for the formation of all activated complexes. Such an equality implies that the isotopic composition of the activated complex is not fractionated relative to the isotopic compositions of atoms and molecules, besides usual mass dependent effects.

3.3.2 The relation between $k_{i,D}(\Theta)$ and $k_D(\Theta)$

We then consider that among all the possible angles at which the activated complex could dissociate, there is only a small fraction of them where it is stabilized via its subsequent reactions with M (see Fig. 5). Therefore, in this model, atoms and molecules that return to the gas do not result from all the scattering angles.

It is possible to relate the $k_{i,D}(\Theta)/k_D(\Theta)$ ratio with the $\beta(\Theta)$ factor defined in the previous section. Assuming

$$d[\mathrm{O}_3^*]/dt = 0 \tag{76}$$

we can write the relations between distinguishable and indistinguishable processes. For this purpose we compare, as an example, the reactions between ^{16}O and ^{17}O^{18}O (i.e. involving only distinguishable species) and between ^{16}O and ^{16}O^{16}O (involving only indistinguishable species)

$$[^{16}\mathrm{O}][^{17}\mathrm{O}^{18}\mathrm{O}]\langle F_T(\theta, v)\rangle = [^{16}\mathrm{O}^{17}\mathrm{O}^{18}\mathrm{O}^*]k_D(\Theta)\,, \tag{77}$$

$$[^{16}\mathrm{O}][^{16}\mathrm{O}^{16}\mathrm{O}]1/2\langle F_T(\theta, v) + F_T(\pi-\theta, v)\rangle = [^{16}\mathrm{O}^{16}\mathrm{O}^{16}\mathrm{O}^*]k_{i,D}(\Theta)\,. \tag{78}$$

Since we assume that no isotopic fractionation took place between the reactants and the activated complex O_3^*

$$[^{16}\mathrm{O}^{17}\mathrm{O}^{18}\mathrm{O}^*]/[^{16}\mathrm{O}^{16}\mathrm{O}^{16}\mathrm{O}^*] = [^{16}\mathrm{O}][^{17}\mathrm{O}^{18}\mathrm{O}]/[^{16}\mathrm{O}][^{16}\mathrm{O}^{16}\mathrm{O}]\,. \tag{79}$$

The relation between $k_{i,D}(\Theta)/k_D(\Theta)$ can then be derived through the ratio (78)/(77)

$$k_{i,D}(\Theta)/k_D(\Theta) = 1/2\langle F_T(\theta, v) + F_T(\pi-\theta, v)\rangle / \langle F_T(\theta, v)\rangle = \beta(\Theta)\,. \tag{80}$$

This formalism will be used hereafter for numerical simulations of the different ozone isotopomer production rates of reactions (57) to (75). From (80) it should not be concluded that, contrary to a previous suggestion by Bates (1988), the life time of the activated complex ^{16}O^{16}O^{16}O* is different from that of ^{16}O^{17}O^{18}O*. As for cross sections, this reflects the fact that it is not possible to distinguish between activated complexes resulting from ^{16}O^{16}O + ^{16}O collisions at scattering angles θ from those at $\pi - \theta$. The numerical values of $\beta(\Theta)$ are estimated in Sect. 4.2.

3.3.3 The constant k_M

No isotopic fractionation is supposed to take place during the stabilization of the complex, and thus k_M is the same for all the isotopically substituted species.

3.4 Formalism for isotopic reaction rates

The partial formation rate of any particular isotopomer (from AAA of reaction (55) to ABB of reaction (75)), can be calculated using (49) with the proper identification of $1/2k^*$, $k_D(\Theta)$, $k_{i,D}(\Theta)$ and $k_\mathrm{M}[\mathrm{M}]$ in place of k^*, $k_D(\Theta)$ and $k_\mathrm{M}[\mathrm{M}]$ appearing in the original Eq. (49). The calculation was performed using the following parameters:

$$K = k_D(\Theta)/k_\mathrm{M}[\mathrm{M}]\,, \tag{81}$$

$$C = (\beta(\Theta)K + 1)/(K + 1)\,. \tag{82}$$

With the rules defined from (55) to (75), the ratio of the isotopic reaction rates can be calculated

$$d[^{16}\mathrm{O}^{16}\mathrm{O}^{17}\mathrm{O}]/d[^{16}\mathrm{O}^{16}\mathrm{O}^{16}\mathrm{O}] = \big\{1/2(1+C)[^{16}\mathrm{O}][^{16}\mathrm{O}^{17}\mathrm{O}] + C[^{17}\mathrm{O}][^{16}\mathrm{O}^{16}\mathrm{O}]\big\} \big/ [^{16}\mathrm{O}][^{16}\mathrm{O}^{16}\mathrm{O}] \tag{83}$$

and similarly with ^{18}O in place of ^{17}O in Eq. (83). In the same manner we have

$$d[^{16}\mathrm{O}^{17}\mathrm{O}^{17}\mathrm{O}]/d[^{16}\mathrm{O}^{16}\mathrm{O}^{16}\mathrm{O}] = \big\{1/2(1+C)[^{17}\mathrm{O}][^{16}\mathrm{O}^{17}\mathrm{O}] + C[^{16}\mathrm{O}][^{17}\mathrm{O}^{17}\mathrm{O}]\big\} \big/ [^{16}\mathrm{O}][^{16}\mathrm{O}^{16}\mathrm{O}] \tag{84}$$

and similarly with ^{18}O in place of ^{17}O in Eq. (84). Finally, for the fully mixed isotopomers, we have

$$d[^{16}\mathrm{O}^{17}\mathrm{O}^{18}\mathrm{O}]/d[^{16}\mathrm{O}^{16}\mathrm{O}^{16}\mathrm{O}] = C\big([^{16}\mathrm{O}][^{17}\mathrm{O}^{18}\mathrm{O}] + [^{17}\mathrm{O}][^{16}\mathrm{O}^{18}\mathrm{O}] + [^{18}\mathrm{O}][^{16}\mathrm{O}^{17}\mathrm{O}]\big) \big/ [^{16}\mathrm{O}][^{16}\mathrm{O}^{16}\mathrm{O}]\,. \tag{85}$$

The density of the isotopic species [O] and [O_2] are calculated statistically

$$[^iO] = [O]x_i \quad (86)$$

$$[^iO^jO] = [O_2]2x_ix_j \quad (87)$$

with x_i and x_j the relative abundance of ^iO and ^jO, respectively with $\sum x_i = 1$. In the next calculation we assume that the gas can be considered as an infinite reservoir relative to ozone, i.e. that the isotopic composition of molecular oxygen remains constant through time.

As far as the parameter y is concerned, it dictates only the final configuration of the ozone molecule. When the isotopic composition of ozone is determined mass spectrometrically, the different isotopomers of ozone (as for example, BAC and ACB) cannot be distinguished and there is no need of taking into account the parameter y. However, in one of the reported laboratory experiments discussed hereafter, the position of the atoms in ozone was determined by Anderson et al. (1989) by infrared spectrometry and related to the isotopic fractionation. Other observations of the symmetrical and non-symmetrical isotopomers of ozone were obtained in the stratosphere by infrared spectroscopy (Goldman et al., 1989). As we will see in the numerical applications, experimental results show that $y \approx 0.1$, indicating that the probability of the incoming atom to be attached to the spectator atom of the molecule is close to unity. Thus, and contrary to other proposed models, the symmetry of the O_3 molecule does not play any special role in the present model.

4 Application to observed isotopic fractionation in ozone

In this section we compare the numerical predictions of the present theory with the observed isotopic fractionation in well defined laboratory systems. For practical purpose a set of formula with the numerical values of the parameters are given in the Appendix. The proper identification of the terms can be derived from Sects. 2 and 3. Numerous experimental papers have been published on the subject of isotopic enhancements in O_3 and we have selected several types of results which represent the most typical and puzzling aspects of this mass independent isotopic fractionation.

4.1 Data basis

We will numerically address the following observations:

(1) The isotopic variations in $^{17}O/^{16}O$ and $^{18}O/^{16}O$ with pressure reported by Thiemens and Jackson (1990). This experiment reproduces two unique features of this mass independent fractionation: (i) contrary to the classical predictions, the fractionation varies with pressure and (ii) almost identical relative variations are observed for both the $^{17}O/^{16}O$ and $^{18}O/^{16}O$ ratios. On the contrary, the "classical" theory of isotopic fractionation predicts a linear correlation with slope 1/2 between the relative variations of the two isotopic ratios.

(2) The plateau in the isotopic fractionation factor observed at low pressure by Morton et al. (1990). This result suggests that the isotopic fractionation factor becomes constant below ca. 100 Torr.

(3) The distribution in the mass range 48 to 54 amu. of ozone isotopic species. This distribution is markedly different from that expected from the classical mass-dependent isotope fractionation theory (Morton et al., 1989; Mauersberger et al., 1993) or from simple statistical distribution of isotopes among O_3. Recently, Sehested et al. (1998) and Mauersberger et al. (1999) reported the rate constants for the different reactions $O + O_2$ involving all the possible permutations between ^{16}O, ^{17}O and ^{18}O. These rates will be compared with the present calculations and will be propagated to the isotopomers of ozone for comparison with the recent data from Wolf et al. (2000).

(4) The asymmetrical ozone molecule $^{16}O^{16}O^{18}O$ which carried more than twice the isotopic enrichment of the symmetrical ozone molecule $^{16}O^{18}O^{16}O$ (Anderson et al., 1989). Similar observations were performed by Christensen et al. (1996), Larsen et al. (2000) and Janssen et al. (1999) for both $^{16}O^{16}O^{18}O$ and $^{16}O^{18}O^{18}O$. These observations are important since in the present theory the isotopic fractionation is independent of the symmetry of the ozone molecule.

We will show that all these results are a possible consequence of the isotopic indistinguishibility.

4.2 Estimation of the β parameter

In the next sections (4.3 to 4.6) $\beta(\Theta)$ is considered as a free parameter and its value is adjusted in order to reproduce the measured isotopic fractionation in ozone. It is nevertheless possible to estimate to what extent $\beta(\theta)$ of (34), i.e. before averaging over Θ, can be different from unity, i.e. different from the "transmission coefficient" which is taken to be equal to 1 in the usual kinetic isotopic fractionation theory (cf. Bigeleisen, 1947). Two limiting cases can be distinguished:
(1) for θ around 0, $F_T(\theta) \gg F_T(\pi - \theta)$; thus $\beta(\theta)$=1/2,
(2) for θ around π, $F_T(\pi - \theta) \gg F_T(\theta)$; thus $\beta(\theta) \gg 1$.

Therefore $\beta(\theta)$ is markedly different from unity for scattering angles around 0 and around π. Note that the average $\beta(\Theta)$ value is exactly equal to unity if the integration is performed between 0 and π and the classical mass-dependent fractionation is restored (see Sect. 2.3). As shown for ozone in the next section, when $\beta(\theta) > 1$ the products of the reaction are enriched in the trace isotopes (such as ^{17}O or ^{18}O in natural oxygen); when $\beta(\theta) < 1$ the products of the reactions exhibit an opposite isotopic fractionation, i.e. they are enriched in the major isotope (such as ^{16}O). For a given reaction, it is therefore not possible to decide "a priori" if this effect yields an anomalous isotopic depletion or enhancement unless a reliable quantum mechanical method is set up to calculate $\beta(\Theta)$ for the range of appropriate formation angles (which is not done here). In the present paper we do not face this problem since we rely on experimental results from which we adjust an empirical value designated hereafter by β.

4.3 Isotopic fractionation with pressure

Mass spectrometric experimental data are from Thiemens and Jackson (1990) and Morton et al. (1990). We have selected the photolysis experiments where ozone was produced in pure O_2. In these experiments no attempt was made by the authors to identify the ozone isotopic species carrying the isotopic anomaly and the $^{17}O/^{16}O$ and $^{18}O/^{16}O$ isotopic ratios represents the bulk value of the mixture of all isotopically substituted ozone molecules.

Since the position of ^{18}O in heavy ozone is irrelevant for mass spectrometry measurements we do not introduce in the calculation the branching ratio y (see Sect. 3.2). In order to be more realistic we have introduced in the calculation two mass-dependent isotopic relations for k^* and β values. They are introduced as

$$k^*_{l-mn} = k^*(\mu_{l-mn}/\mu_{16-1616})^a \,. \tag{88}$$

μ is the reduced mass for $O - O_2$, l, m and n stand for mass 16, 17 or 18, l stands for atoms, mn for molecules. The parameter a is usually taken equal to $-1/2$ or $-1/3$. This gives the usual mass-dependent relationship

$$k^*_{17-1616} = k^*(1+\varepsilon_k) \quad \text{and} \quad k^*_{18-1616} \cong k^*(1+2\varepsilon_k) \,. \tag{89}$$

ε designates the isotopic fractionation factor expressed per mass unit. The same treatment was applied for β (hence the notation ε_β). The isotopic composition of ozone in a given experiment is expressed in the usual δ units

$$\delta^i\mathrm{O}(‰) = [(^i\mathrm{O}/^{16}\mathrm{O})_{\text{experiment}}/(^i\mathrm{O}/^{16}\mathrm{O})_{\text{statistic}} - 1] \times 1000 \tag{90}$$

Such a treatment allows the calculation of the slope s defined by the linear relation between δ^{17}O(‰) and δ^{18}O(‰) in the three isotope diagram: $s = \Delta(\delta^{17}\mathrm{O})/\Delta(\delta^{18}\mathrm{O})$. For the mass-dependent isotopic fractionation ($\beta = 1$), the slope s is calculated with the present theory to vary between 0.514 and 0.529 for δ^{17}O varying between +50‰ and −50‰, respectively. These numerical results are in excellent agreement with values measured by several authors (Clayton et al. 1973; Robert et al., 1992; Meier and Li, 1998).

The calculations of the isotopic composition of ozone as a function of pressure are reported in Figs. 6a, b. They were performed by adjusting the model parameters to the experimental results. That is $k_D(\Theta)/k_\mathrm{M} = 10^{20}$, $\beta = 1.15$, $\varepsilon_k = -10‰$, $\varepsilon_\beta = +32‰$. The variation with pressure of the parameter K ($K = k_D(\Theta)/k_\mathrm{M}[\mathrm{M}]$) was calculated rigorously, i.e. using the proper equation of state for gaseous molecular oxygen to determine [M] as a function of the pressure P_{O_2}. It should be noted that the final isotopic composition of ozone depends strongly on the actual value of β while the three other parameters do not affect this isotopic composition by more than a few per mil. Taking a numerical example of such relations between parameters, a change from 1.15 to 1.16 in the β value yields roughly an isotopic effect of 10‰.

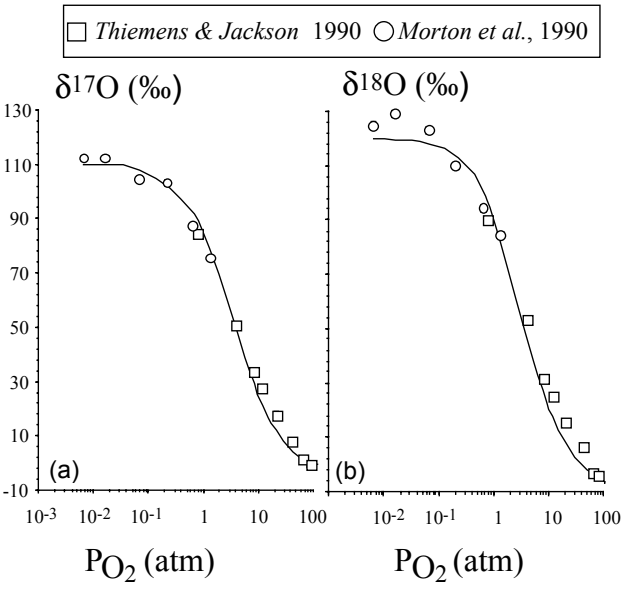

Fig. 6. Calculated variations (solid lines) of **(a)** δ^{17}O(‰) and **(b)** δ^{18}O(‰) as a function of pressure. Experimental data are from Thiemens and Jackson (1990) and Morton et al. (1990).

At a first order of approximation, the value of the ratio $k_D(\Theta)/k_\mathrm{M} = 10^{20}$ molecule cm^{-3} which fits the isotopic variations as a function of pressure, is consistent with the previous estimates published in the literature. In the notations of Kaufman and Kelso (1967), $k_D(\Theta)/k_\mathrm{M}$ is noted k_b/k_c with $k_b = 3{\cdot}10^{10}$ s^{-1} and $k_c = 1{\cdot}10^{-11}$ cm^3 molecule^{-1} s^{-1} preferred by these authors to those of Klein and Herron (1966), i.e. $k_b = 1.8{\cdot}10^9$ s^{-1} and $k_c = 7{\cdot}10^{-13}$ cm^3 molecule^{-1} s^{-1}. The corresponding values of k_b/k_c are $3 \cdot 10^{21}$ and $2.6 \cdot 10^{21}$, respectively. Although k_b and k_c vary by more than one order of magnitude, these authors choose the same value for k_a (k^* in our notation, i.e. $k^*k_D(\Theta)/k_\mathrm{M} = k_a k_b/k_c$) yielding identical k_b/k_c ratios. Considering the whole range of variations of k_b and k_c measured by these authors, a k_b/k_c ratio ranging between $1.8 \cdot 10^{20}$ and $4 \cdot 10^{22}$ seems possible, hence compatible with $1 \cdot 10^{20}$ calculated here.

At a second order of approximation an interesting effect may be related to the difference between $k_D(\Theta)/k_\mathrm{M}$ and k_b/k_c. As proposed by Pack et al. (1998), several types of activated complexes seem to exist in three body reactions. It could then be admitted that the activated complex, involved in the angular isotopic effect described here, has a k^* value different from that determined through the low pressure approximation (see Eq. 50).

Several observations are reproduced by this model (see Figs. 6a, b): 1) the plateau for δ^mO values at low pressure 2) the pressure dependence and 3) the cross over in the $^{17}O/^{16}O - ^{18}O/^{16}O$ isotopic fractionation around 1 atm: $\delta^{18}\mathrm{O} > \delta^{17}\mathrm{O}$ at low pressure and $\delta^{18}\mathrm{O} < \delta^{17}\mathrm{O}$ at high pressure. The maxima of δ^{17}O and δ^{18}O are dictated by the value of β while the parameter K dictates the shape of the functions δ^mO versus pressure. The two sets of experiments at

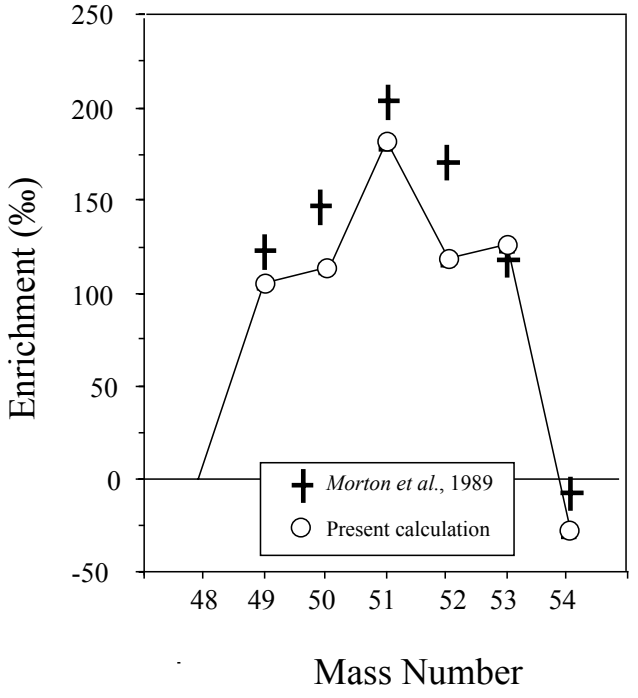

Fig. 7. Calculated enhancements in the different isotopically substituted ozone molecules (from $^{17}O^{16}O^{16}O$ to $^{18}O^{18}O^{18}O$; mass 49 to 54) are compared with experimental data (Morton et al., 1989).

low and high pressure were performed by different laboratories. Since they are reproduced numerically for the same value of the parameters, these parameters are used for all the following calculations.

4.4 Non mass-dependent fractionation in ozone isotopomers

Morton et al. (1989) and Mauersberger et al. (1993) recorded the isotopic fractionation linked to the isotopic substitution in O_3. These data are compared in Fig. 7 with the theoretical predictions of the present model using the previously determined parameters for β, ε_k, ε_β and K. The isotopic abundances and the pressure correspond to the experimental conditions indicated by Morton et al. (1989) in their paper. As observed in Fig. 7 the marked enhancement in the $^{16}O^{17}O^{18}O/^{16}O^{16}O^{16}O$ ratio (at mass 51 in the figure) relative to the other isotopically substituted species is qualitatively reproduced by the calculation, as well as the intermediate enhancement at masses 49, 50 , 52 and 53. However, the theoretical pattern is systematically lower than the experimental data. This can be understood as follows.

In the experiment reported by Morton et al. (1989), ozone was formed by an electric discharge while the different parameters β_k, ε_k, ε_β and K were determined in Sect. 4.3 for ozone produced by photolysis (Thiemens and Jackson, 1990; Morton et al., 1990). Therefore, it is conceivable that the parameter β is also linked to different experimental techniques to generate ozone. For example, if β is adjusted to 1.17 (instead of 1.15 used here), the calculated enhancements for all the species translate upward and match almost exactly the mass 49, 50, 51 and 52.

Table 1. Comparison between observed and calculated isotopic fractionation in ozone isotopomer (expressed in per mil) produced by photolysis. Data are from Mauersberger et al. (1993). The parameters of the calculation are defined in Sect. 4.3. Parameters: $\beta = 1.15$, $a = -0.25$, $b = 0.80$, $c = 0$, $P = 100$ Torr; see appendix

		Enrichment (‰)		
Mass	Species	Observed	Calculated	Difference
48	$^{16}O^{16}O^{16}O$	$\equiv 0$	$\equiv 0$	
49	$^{16}O^{16}O^{17}O$	113	109	−4
50	$^{16}O^{17}O^{17}O$	121	110	−11
50	$^{16}O^{16}O^{18}O$	130	118	−12
51	$^{16}O^{17}O^{18}O$	181	186	+5
51	$^{17}O^{17}O^{17}O$	−18	−15	+3
52	$^{16}O^{18}O^{18}O$	144	120	−24
52	$^{17}O^{17}O^{18}O$	95	129	+34
53	$^{17}O^{18}O^{18}O$	83	130	+47
54	$^{18}O^{18}O^{18}O$	−46	−29	+17

Table 2. Comparison between the rate constants measured by Sehested et al. (1998) with the calculations using the parameters given in Sect. 4.3. $^{16}O+^{16}O^{16}O$ (k_1), $^{18}O+^{16}O^{16}O$ (k_2) and $^{16}O+^{18}O^{18}O$ (k_3), $^{16}O+^{16}O^{18}O$ (k_4) and $^{18}O+^{16}O^{18}O$ (k_5), $^{18}O+^{18}O^{18}O$ (k_6)

	Sehested et al. (1998)	Present calculation
$(k_2+k_3)/2k_1$	1.184±0.037	1.185
$(k_4+k_5)/2k_1$	1.155±0.062	1.086
k_6/k_1	0.977±0.021	0.977

A similar experiment has been repeated by Mauersberger et al. (1993) for photolysis experiments and the isobaric interferences at mass 50, 51 and 52 were estimated. These experimental results are reported in Table 1 and compared with our theoretical calculations using the previously determined β, ε_k, ε_β and K parameters. This comparison reveals several encouraging points: (1) the theoretical and observed isotopic fractionation for the mass dependent fractionated species $^{17}O^{17}O^{17}O$ and $^{18}O^{18}O^{18}O$ are in agreement within ±15‰, (2) the theoretical and the observed isotopic fractionation for the anomalously fractionated species at mass 49 to 51 are in agreement within ±8‰, (3) at higher masses, and especially for the two species $^{17}O^{17}O^{18}O$ and $^{17}O^{18}O^{18}O$, the experimental isotopic fractionation is about 35‰ lower than calculated. This point will be addressed in Sect. 4.5. However, according to our calculation, these effects contribute at most for 30% of the net effect.

Sehested et al. (1998) have determined the rate constants

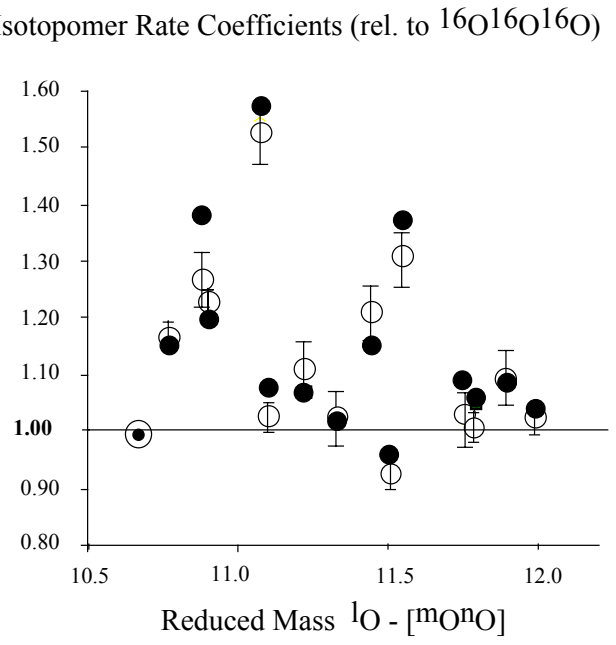

Fig. 8. Specific rates coefficients for isotopomer as a function of the reduced mass for the reactions ${}^{l}\mathrm{O}+{}^{m}\mathrm{O}{}^{n}\mathrm{O}$ (l, m and n stand for mass 16, 17 or 18). Data (open disks) from Mauersberger et al. (1999) are shown with their error bars and calculated values are in black. The calculation is performed in the low pressure approximation with $a = +0.3$, $b = -3.5$, $c = +10$ and $\beta = 1.20$; see appendix.

for the reactions ${}^{16}\mathrm{O} + {}^{16}\mathrm{O}{}^{16}\mathrm{O}$ (k_1), ${}^{18}\mathrm{O} + {}^{16}\mathrm{O}{}^{16}\mathrm{O}$ (k_2) and ${}^{16}\mathrm{O} + {}^{18}\mathrm{O}{}^{18}\mathrm{O}$ (k_3), ${}^{16}\mathrm{O} + {}^{16}\mathrm{O}{}^{18}\mathrm{O}$ (k_4) and ${}^{18}\mathrm{O} + {}^{16}\mathrm{O}{}^{18}\mathrm{O}$ (k_5), ${}^{18}\mathrm{O} + {}^{18}\mathrm{O}{}^{18}\mathrm{O}$ (k_6). For these reactions, the results of our calculated rate constants are reported in Table 2 and compared with those of Sehested et al. The calculations are in perfect agreement for the reactions involving only distinguishable isotopes (i.e. ${}^{18}\mathrm{O} + {}^{16}\mathrm{O}{}^{16}\mathrm{O}$ and ${}^{16}\mathrm{O} + {}^{18}\mathrm{O}{}^{18}\mathrm{O}$) or only indistinguishable isotopes (i.e. ${}^{18}\mathrm{O} + {}^{18}\mathrm{O}{}^{18}\mathrm{O}$). However for the reactions involving one distinguishable and one indistinguishable isotopes (i.e. ${}^{16}\mathrm{O} + {}^{16}\mathrm{O}{}^{18}\mathrm{O}$ and ${}^{18}\mathrm{O} + {}^{16}\mathrm{O}{}^{18}\mathrm{O}$), the calculated rate constants are in slight disagreement with observations (1.086 and 1.155 ± 0.062 respectively). Note that the experimental result is also in agreement with the reactions rates measured or derived by Mauersberger et al. (1999). We will see in the next section that the disagreement is caused by the reaction ${}^{16}\mathrm{O} + {}^{16}\mathrm{O}{}^{18}\mathrm{O}$ whose calculated rate is 1.19 while its measured rate is 1.27. This may be caused by an additional isotopic effect of the symmetrical relative to the asymmetrical variant of the molecule which is not modeled in the present theory.

4.5 Isotopomer specific rate coefficients

Contrary to the first order of approximation used in Sects. 4.3 and 4.4 according to which the value of β is equal for all types of reactions between O and O_2, the results obtained by Mauersberger et al. (1999) put into light another property of β: its value is also mass-dependently related with the mass of the molecule involved in the isotopic reaction. As for reaction (88), this relation can be written as

$$\beta_{mn-16} = \beta(\mu_{16-mn}/\mu_{16-1616})^c \,. \tag{91}$$

This dependence is different from that illustrated by reaction (88) describing the relation of β with the reduced mass of the reactants. As a whole, β can be written

$$\beta_{mn-l} = \beta(\mu_{16-mn}/\mu_{16-1616})^c(\mu_{l-mn}/\mu_{16-1616})^b \tag{92}$$

(as in (88) l, m, n designates 16, 17 ,18 and l stands for atoms and mn for molecules). Therefore, in this theory, the only non classical (i.e. non mass-dependent) parameter is β, i.e. the rate constant ratio describing the reactions between distinguishable and undistinguishable isotopes. The mass-dependent parameters a, b, and c were adjusted to the following values: $a = +0.3$, $b = -3.4$ and $c = +10$, corresponding to 15‰/amu, −130‰/amu and +105‰/amu, respectively. Numerical results are reported in Table 3 for $\beta = 1.22$ and reproduce within ±3% the data reported by Mauersberger et al. (1999). These results are also reported in Fig. 8 as a function of the reduced mass of the reactants for the individual rates ${}^{l}\mathrm{O}+{}^{m}\mathrm{O}{}^{n}\mathrm{O}$.

From these individual rates, the isotopic compositions of the isotopomers obtained in scrambled mixtures can be calculated and compared with the recent results of Wolf et al. (2000) obtained at 60 Torr. However there is one difficulty

Table 3. Isotopomer specific rate coefficients calculated with the parameters defined in the appendix and having the values $\beta = 1.22$, $a = 0.3$, $b = -3.4$, $c = 10$, $P = 0$ Torr. Measured rates are from Mauersberger et al. (1999)

Reactions	Calculated Rate	Measured Rate	Reduced Mass
${}^{16}\mathrm{O}+{}^{16}\mathrm{O}{}^{16}\mathrm{O}$	$\equiv 1$	$\equiv 1$	10.67
${}^{17}\mathrm{O}+{}^{16}\mathrm{O}{}^{16}\mathrm{O}$	1.08	1.03	11.10
${}^{18}\mathrm{O}+{}^{16}\mathrm{O}{}^{16}\mathrm{O}$	0.96	0.93	11.52
${}^{16}\mathrm{O}+{}^{17}\mathrm{O}{}^{17}\mathrm{O}$	1.39	1.23	10.88
${}^{17}\mathrm{O}+{}^{17}\mathrm{O}{}^{17}\mathrm{O}$	1.02	1.02	11.33
${}^{18}\mathrm{O}+{}^{17}\mathrm{O}{}^{17}\mathrm{O}$	1.10	1.03	11.77
${}^{16}\mathrm{O}+{}^{18}\mathrm{O}{}^{18}\mathrm{O}$	1.58	1.53	11.08
${}^{17}\mathrm{O}+{}^{18}\mathrm{O}{}^{18}\mathrm{O}$	1.39	1.31	11.55
${}^{18}\mathrm{O}+{}^{18}\mathrm{O}{}^{18}\mathrm{O}$	1.04	1.03	12.00
${}^{16}\mathrm{O}+{}^{16}\mathrm{O}{}^{17}\mathrm{O}$	1.15	1.17	10.78
${}^{17}\mathrm{O}+{}^{16}\mathrm{O}{}^{17}\mathrm{O}$	1.08	1.11	11.22
${}^{18}\mathrm{O}+{}^{16}\mathrm{O}{}^{17}\mathrm{O}$	1.03	nd	11.65
${}^{16}\mathrm{O}+{}^{16}\mathrm{O}{}^{18}\mathrm{O}$	1.20	1.27	10.88
${}^{17}\mathrm{O}+{}^{16}\mathrm{O}{}^{18}\mathrm{O}$	1.23	nd	11.33
${}^{18}\mathrm{O}+{}^{16}\mathrm{O}{}^{18}\mathrm{O}$	1.06	1.01	11.77
${}^{16}\mathrm{O}+{}^{17}\mathrm{O}{}^{18}\mathrm{O}$	1.49	nd	10.98
${}^{17}\mathrm{O}+{}^{17}\mathrm{O}{}^{18}\mathrm{O}$	1.16	1.21	11.44
${}^{18}\mathrm{O}+{}^{17}\mathrm{O}{}^{18}\mathrm{O}$	1.10	1.09	11.89

Table 4. Comparison between calculations performed for isotopically non-fractionated (column 1) and fractionated (column 2) oxygen atoms in a scrambled gas. The calculations were performed at 60 Torr with the parameters reproducing the isotopomer specific rate coefficients (Mauersberger et al., 1999; cf. Table 3). Recent data at 60 Torr on all ozone isotopomers are reported for comparison (Wolf et al., 2000). The difference between the results in column 2 and the measured isotopic composition are reported in the last column (Δ)

		Enrichment (‰)			
Mass	Species	Column 1 Calculated	Column 2 Calculated	Measured	Δ
48	$^{16}O^{16}O^{16}O$	$\equiv 0$	$\equiv 0$	$\equiv 0$	$\equiv 0$
49	$^{16}O^{16}O^{17}O$	129	114	106	8
50	$^{16}O^{17}O^{17}O$	188	159	110	49
50	$^{16}O^{16}O^{18}O$	121	96	130	−34
51	$^{16}O^{17}O^{18}O$	248	206	198	8
51	$^{17}O^{17}O^{17}O$	18	−22	−15	−7
52	$^{16}O^{18}O^{18}O$	234	180	161	19
52	$^{17}O^{17}O^{18}O$	142	83	94	−11
53	$^{17}O^{18}O^{18}O$	195	121	89	32
54	$^{18}O^{18}O^{18}O$	36	−43	−39	−4

with this calculation. In two cases, an individual rate (cf. Table 3) is directly comparable with the isotopic composition of an isotopomer obtained in scrambled mixtures: this is the case for $^{18}O^{18}O^{18}O$ (and similarly for $^{17}O^{17}O^{17}O$) which can result from only one reaction, i.e. $^{18}O + {}^{18}O^{18}O$. The measured reaction rate in pure ^{18}O for $^{18}O + {}^{18}O^{18}O$ is +30‰ (i.e. 1.03 in Table 4) while in scrambled mixtures the isotopomer $^{18}O^{18}O^{18}O$ is fractionated by ≈ -40‰ (corresponding to 0.96), i.e. by −70‰ relative to the predicted value of +30‰. As suggested by Mauersberger in reviewing the present article, isotope exchange reactions are fast and, under equilibrium, the $^{18}O/^{16}O$ atomic oxygen ratio should be 76‰ relative to the statistical composition of the mixture (Anderson et al., 1997). Such an isotopic fractionation of atoms has been introduced in the present calculations and was mass-dependently propagated for all the reactions contributing to the formation of all the isotopomers. This effect can also be reproduced within the framework of the present theory by replacing the parameter $a = 0.30$ in Eq. (88) by $a = -0.36$. Results are reported in Table 4 and compared with the results expected without taking into account this effect.

From Table 4, it can be verified that, taking into account the isotopic fractionation of oxygen atoms in the gas, theoretical and experimental results become closer. On average, the absolute differences between the calculated and the measured $\delta^{18}O$ values of the different isotopomers are within ±20‰. However they are not statistically distributed around zero. For example, the differences are still large for $^{16}O^{16}O^{18}O$ (−34‰), $^{16}O^{17}O^{17}O$ (+49‰) and $^{17}O^{18}O^{18}O$ (+32‰) (cf. Table 4; remember that symmetrical and unsymmetrical variants are not separated in mass spectrometry) while, for other species, they are smaller than 20‰. This departure between theoretical and experimental enrichments is not statistically different from what was obtained for calculated individual rates and, in this respect, likely represents the highest degree of approximation which can be reached by the present theory.

Table 5. Exit channel specific rate coefficients for the formation of $^{50}O_3$ and $^{52}O_3$. The parameters of the calculations are defined in appendix and determined from specific rates coefficients (see Table 3): $\beta = 1.2$, $a = 0.3$, $b = -3.5$, $c = 10$, $P = 0$ Torr. The probability for an incoming atom to be attached to the knock-on atom of the O_2 molecule is designated by y. Measured ratios are from Janssen et al. (1999)

Reactions	Calculated Ratio		Measured
	$y = 0.5$	$y = 0.1$	Ratio
$^{16}O+{}^{16}O^{18}O \rightarrow {}^{16}O^{16}O^{18}O$	1.19	1.33	1.45±0.04
$^{16}O+{}^{18}O^{16}O \rightarrow {}^{16}O^{18}O^{16}O$	1.19	1.04	1.08±0.01
$^{18}O+{}^{16}O^{16}O \rightarrow {}^{18}O^{16}O^{16}O$	0.94	0.94	0.92±0.04
$^{18}O+{}^{16}O^{16}O \rightarrow {}^{16}O^{18}O^{16}O$	0.0	0.0	0.006±0.005
$^{18}O+{}^{18}O^{16}O \rightarrow {}^{18}O^{18}O^{16}O$	1.05	1.06	0.92±0.06
$^{18}O+{}^{16}O^{18}O \rightarrow {}^{18}O^{16}O^{18}O$	1.05	1.03	1.04±0.02
$^{16}O+{}^{18}O^{18}O \rightarrow {}^{16}O^{18}O^{18}O$	1.55	1.55	1.50±0.03
$^{16}O+{}^{18}O^{18}O \rightarrow {}^{18}O^{16}O^{18}O$	0.0	0.0	0.029±0.006

4.6 Isotopomer fractionation ratio

Anderson et al. (1989) reported the ratio $R_1 = [^{16}O^{16}O^{18}O]/[^{16}O^{18}O^{16}O]$ which ranges from 2.27 to 2.19 according to the highest and lowest isotopic enrichment levels, respectively, that could be achieved in their experiment (ozone being produced by electric discharge). Larsen et al. (2000) have reported the determination of the ratio $R_2 = [^{16}O^{18}O^{18}O]/[^{18}O^{16}O^{18}O]$ along with R_1: within the uncertainties of the measurements, R_1 cannot be distinguished from its classical value of 2.0, while R_2 lies between 2.42 and 2.52. Janssen et al. (1999) reported the four possible rates yielding to $^{16}O^{16}O^{18}O$ and $^{16}O^{18}O^{16}O$ along with the four possible rates yielding to $^{16}O^{18}O^{18}O$ and $^{18}O^{16}O^{18}O$. The corresponding R_1 and R_2 ($R_1 = 2.75$ and $R_2 = 2.33$) are different from Anderson et al. (1989) and also different from Larsen et al. (2000).

Since the determinations of Janssen et al., (1999) have been obtained under the same experimental conditions than those for the individual rate constants reported by Mauersberger et al. (1999), the calculations were performed using the parameters determined in Sect. 4.5 (see Fig. 8). Results are reported in Table 5. The agreement between theoretical and experimental values is satisfying. Small but significant differences between experimental and theoretical values still exists, however, for the two reactions $^{16}O + {}^{16}O^{18}O$. These differences may be accounted for by the appropriate value of

the parameter y, i.e. the probability for an incoming atom to be attached to the knock-on atom of the O_2 molecule (see Eq. 58). In Table 5, calculations are reported for $y = 1/2$ and $y = 0.1$. For $y = 0.1$ the numerical results are in close agreement with the determinations of Janssen et al. (1999).

Note that the departure of R_1 from its classical value of 2 is entirely due to the reaction between indistinguishable isotopes. If this reaction is ignored (i.e. if $\beta = 1$, $b = 0$, $c = 0$) the ratio of the two isotopomers is exactly 2.00 ± 0.03 whatever the values of all the other parameters.

4.7 Isotopic fractionation with temperature

Morton et al. (1990) have reported the isotopic fractionation of ozone as a function of temperature. The variation with temperature of the rate constants involved in the formation of ozone has been established in the literature (see DeMore et al., 1997). Introducing these numerical results in the present theory (see Eq. 53) does not yield the results obtained by Morton et al. (1990) for the isotopic fractionation. This may indicate that the parameter β also depends on the temperature. If this interpretation is correct, such a relation between β and the temperature can be understood as follows: the scattering angles at which ozone is stabilized vary with temperature, i.e. with the internal energy at which the activated complex is formed. No attempt was made here to take into account this dependence.

5 Conclusions

Hathorn and Marcus (1999) have proposed another interpretation of the oxygen isotope effect in ozone based on the fact that the asymmetric ozone isotopomers have a larger density of reactive states compared with that for symmetric species. Therefore, the role played by the molecular symmetry in this isotopic effect should be used to test these two theories.

The theory presented here could be experimentally tested through several types of experiments: (1) a cross beam experiment where the isotopic compositions of the scattered products are recorded as a function of their scattering angles, (2) a bulk absorption experiment of an atomic beam by a buffer gas where the isotopic composition of the outcoming beam is measured, (3) a scattering experiment of a keV beam through a solid thin target where the isotopic compositions of atoms crossing the target are measured.

Since it seems possible that the difference in the scattering cross sections involving distinguishable and indistinguishable isotopes is the central parameter which dictates the final anomalous isotopic composition of ozone, oxygen isotopic anomalies in other chemical reactions or isotopic anomalies in other chemical elements may also result from this effect.

Acknowledgements. Constructive reviews accompanied by informal discussions by e-mail with M. Thiemens and K. Mauersberger have led to marked improvements of this paper. They are both deeply acknowledged. One of us (FR) wish to thank the positive attitude of his colleagues at CRPG-Nancy, along with S. Epstein, J. Micallef and P. Richet, which was of great help. This work was supported by grants from the Musum-Paris, CNES, PCMI, PNCA, and PNP-INSU.

Topical Editor J.-P. Duvel thanks M. H. Thiemens and another referee for their help in evaluating this paper.

Appendix

Formula

$$(\mu_{l-mn})^a/(\mu_{16-1616})^a = \Delta\mu^a$$
$$(\mu_{l-mn})^b/(\mu_{16-1616})^b = \Delta\mu^b$$
$$(\mu_{16-mn})^c/(\mu_{16-1616})^c = \Delta\mu^c$$
$$\beta^* = \beta\Delta\mu^b\Delta\mu^c$$
$$C = (\beta^* K + 1)/(K + 1)$$
$$K = k_D(\Theta)/k_{\mathrm{M}}[\mathrm{M}]$$

Rate coefficients relative to the standard rate $^{16}O + ^{32}O_2$ (low pressure approximation)

If $l = m = n$:	$k_{l-mn}/k_{16-1616} = \Delta\mu^a$
If $l \neq m = n$ or $l \neq m \neq n$:	$k_{l-mn}/k_{16-1616} = C\Delta\mu^a$
If $l = m \neq n$:	$k_{l-mn}/k_{16-1616} = 1/2(1 + C)\Delta\mu^a$

l, m and n stand for mass 16, 17 or 18, l for atoms and mn for molecules.

Numerical values

$$k_D(\Theta)/k_{\mathrm{M}} = 10^{20}$$
$$\beta = 1.22,\ a = +0.3,\ b = -3.4,\ c = +10$$

References

Abbas, M. M., Guo, J., Garli, B., Mencaraglia, F., Carlotti, M., and Nolt, I. G., Heavy ozone distribution in the stratosphere from far-infrared observations, J. Geophys. Res., 92, 13231–13239, 1987.

Anderson, S. M., Klein, F. S., and Kaufmann, F., Kinetics of the isotope exchange reaction of ^{18}O with NO and O_2 at 298 K, J. Chem. Phys., 83, 1648–1656, 1985.

Anderson, S. M., Morton, J., and Mauersberger, K., Laboratory measurements of ozone isotopomers by tunable diode laser absorption spectroscopy, Chem. Phys. Lett., 156, 175–180, 1989.

Anderson, S. M., Mauersberger, K., Morton, J., and Schueler, B., Heavy ozone anomaly – Evidence for a mysterious mechanism, in Gas-Phase Chemistry, Ed. J. A. Kaye, 502, Am. Chem. Soc., Washington, pp. 155–166, 1991.

Anderson, S. M. and Mauersberger, K., Ozone absorption spectroscopy in search of low-lying electronic states, Chem. Phys. Lett., 100, 3033–3048, 1995.

Anderson, S. M., Hülselbusch, D., and Mauersberger, K., Surprising rate coefficients for four isotopic variants of $O + O_2 + M$, J. Chem. Phys., 107, 5385–5392, 1997.

Bahou, M., Schriver-Mazzuoli, L., Camy-Peyret, C., and Schriver, A., Photolysis of ozone at 693 nm in solid oxygen. Isotopic effects in ozone reformation, Chem. Phys. Letters, 273, 31–36, 1997.

Bates, D. R., Suggested explanation of heavy ozone, Geophys. Res. Lett., 15, 13–16, 1988.

Bigeleisen, J., The relative reaction velocities of isotopic molecules, J. Chem. Phys., 17, 675–678, 1949.

Christensen, L. K., Larsen, N. W., Nicolaisen, F. M., Pedersen, T., Sørensen, G. O., and Egsgaard, H., Far-IR spectroscopy of ozone as a means of quantification of ozone isotopomers, J. Mol. Spectrosc., 175, 220–333, 1996.

Cicerone, R. J. and McCrumb, J. L., Photodissociation of isotopically heavy O_2 as a source of atmospheric O_3, Geophys. Res. Lett., 7, 251–254, 1980.

Clayton, R. N., Grossman, L., and Mayeda, T. K., A component of primitive nuclear composition in carbonaceous meteorites, Science, 182, 485–488, 1973.

Colman, J. J., Xianping, X., Thiemens, M. H., and Trogler, W. C., Photopolymerization and mass-independent sulfur isotope fractionations in carbon disulfide, Science, 273, 774–776, 1996.

DeMore, W. B., Sander, S. P., Golden, D. M., Hampson, R. F., Kurylo, M. J., Howard, C. J., Ravishankara, A. R., Kolb, C. E., and Molina, M. J., Chemical kinetics and photochemical data for use in stratospheric model, JPL publication, 97-4, Jet Propul. Lab., Pasadena, 1997.

Gellene, G. I., An explanation for symmetry-induced isotopic fractionation in ozone, Science, 274, 1344–1346, 1996.

Goldman, A., Murcray, F. J., Murcray, D. G., Kosters, J. J., Rinsland, C. P., Flaud, J.-M., Camy-Peyret, C., and Barbe, A., Isotopic abundances of stratospheric ozone from balloon-borne high-resolution infrared solar spectra, J. Geophys. Res., 94, 8467–8473, 1989.

Goldman, A., Schoenfeld, W. G., Stephen, T. M., Murcray, F. J., Rinsland, C. P., Barbe, A., Hamdouni, A., Flaud, J.-M., and Camy-Peyret, C., Isotopic ozone in the 5μ region from high resolution balloon-borne and ground-based FTIR solar spectra, J. Quant. Spectroscopy. Radiative Transfer, 59, 231–244 1998.

Hathorn, B. C. and Marcus, R. A. An intramolecular theory of the mass-independent isotope effect for ozone, J. Chem. Phys., Vol. III, 9, 4087–4100, 1999.

Heidenreich III, J. E. and Thiemens, M. H. J., A non-mass-dependent oxygen isotope effect in the production of ozone from molecular oxygen: the role of molecular symmetry in isotope chemistry, Chem. Phys., 84, 2129–2136, 1986.

Janssen, C., Guenther, J., Krankowsky, D., and Mauersberger, K., Relative formation rates of $^{50}O_3$ and $^{52}O_3$ in $^{16}O - ^{18}O$ mixtures, J. Chem. Phys., III, 7179–7182, 1999.

Kaufman, F. and Kelso, J. R., M effect in the gas-phase recombination of O with O_2, J. Chem. Phys, 46, 4541–4543 1967.

Kaye, J. A. and Strobel, D. F., Enhancement of heavy ozone in the Earth's atmosphere? J. Geophys. Res., 88, 8447–8452, 1983.

Kaye, J. A., Theoretical analysis of isotope effects on ozone formation in oxygen photochemistry, J. Geophys. Res., 91, 7865–7874, 1986.

Klein, F .S. and Herron, J. T., Erratum: Mass-spectrometric study of the reaction of O atoms with NO and NO_2, J. Chem. Phys., 44, 3645–3646, 1966.

Krankowsky, D., Lämmerzahl, P., and Mauersberger, K., Isotopic measurements of stratospheric ozone, Geophys. Res. Lett., 27, 2593–2595, 2000.

Larsen, R. W., N.W. Larsen, N. W., F.M. Nicolaisen, F. M., G.O. Sørensen, G. O., and Beukes, J. A., Measurements of ^{18}O-enriched ozone isotopomer abundances using high-resolution Fourier transform far-IR spectroscopy, J. Mol. Spectrosc., 200, 235–247, 2000.

Mauersberger, K., Measurements of heavy ozone in the stratosphere, Geophys. Res. Lett., 8, 935–937, 1981.

Mauersberger, K., Ozone isotope measurements in the stratosphere, Geophys. Res. Lett., 14, 80–83, 1987.

Mauersberger, K., Morton, J., Schueler, B., Stehr, J., and Anderson, S. M., Multi-isotope study of ozone: implications for the heavy ozone anomaly, Geophys. Res. Lett., 20, 1031–1034, 1993.

Mauersberger, K., Erbacher, B., Krankowsky, D., Günther, J., and Nickel, R., Ozone isotope enrichment: isotopomer-specific rate coefficients, Science, 283, 370–372, 1999.

Meijer, H. A. J. and Li, W. J., The use of electrolysis for accurate $\delta^{17}O$ and $\delta^{18}O$ isotope measurements in water, Isotopes Environ. Health Stud., 34, 349–369, 1998.

Morton, J., Schueler, B., and Mauersberger, K., Oxygen fractionation of ozone isotopes $^{48}O_3$ through $^{54}O_3$, Chem. Phys. Lett., 154, 143–145, 1989.

Morton, J., Barnes, I., Schueler, B, and Mauersberger, K., Laboratory studies of heavy ozone, J. Geophys. Res., 95, 901–907, 1990.

Pack, R. T., Walker, R. B., and Kendrick, B. K., Three-body collision contributions to recombination and collision-induced dissociation. II. Kinetics, J. Chem. Phys, 109, 6714–6724, 1998.

Robert, F., Halbout, J., and Baudon, J., A non-mass-dependent isotopic fractionation effect, Earth. Planet. Sci. Lett., 91, 231–238, 1988.

Robert, F. and Baudon, J., Reply to comment by M. Sund on "A non mass-dependent isotopic fractionation effect", Earth. Planet. Sci. Lett., 98, 402–404, 1990.

Robert, F., Rejou-Michel, A., and Javoy, M., Oxygen isotopic homogeneity of the Earth: new evidences, Earth Planet. Sci. Lett., 108, 1–9, 1992.

Schueler, B., Morton, J., and Mauersberger, K., Measurements of isotopic abundance in collected ozone samples, Geophys. Res. Lett., 17, 1295–1299, 1990.

Sehested, J., Nielsen, O. J., Egsgaard, H., Larsen, N. W., Pedersen, T., Christensen, L. K., and Wiegell, M., First direct kinetic study of isotopic enrichment of ozone, J. Geophys. Res., 100, 20979–20982, 1995.

Sehested, J., Nielsen, O. J., Egsgaard, H., Larsen, N. W., Andersen, T. S., and Pedersen, T., Kinetic study of the formation of isotopically substituted ozone in argon, J. Geophys. Res., 103, 3545–3552, 1998.

Thiemens, M. H. and Heidenreich III, J. E., The mass-independent fractionation of oxygen: a novel isotope effect and its possible cosmological implications, Science, 219, 1013–1075, 1983.

Thiemens, M. H. and Jackson, T., Production of isotopically heavy ozone by ultraviolet light photolysis of O_2, Geophys. Res. Lett., 14, 624–627, 1987.

Thiemens, M. H. and Jackson, T., Pressure dependency for heavy isotope enhancement in ozone formation, Geophys. Res. Lett., 17, 717–719, 1990.

Thiemens, M., Mass-independent isotope effects in planetary atmospheres and the early solar system, Science, 283, 341–346, 1999.

Urey, H. C., The thermodynamic properties of isotopic substances, J. Chem. Soc., 562–569, 1947.

Valentini, J. J., Mass-independent isotopic fractionation in nonadiabatic molecular collisions, J. Chem. Phys., 86, 6757–6765, 1987.

Wolf, S., Bitter, M., Krankowsky, D., and Mauersberger, K., Multi-isotope study of fractionation effects in the ozone formation process, J. Chem. Phys., 113, 7, 2684–2686, 2000.

Yang, J. and Epstein, S., The effect of isotopic composition of oxygen on the non-mass-dependent isotopic fractionation in the formation of ozone by discharge of O_2^*, Geochim. Cosmochim. Acta, 51, 2011–2017, 1987.